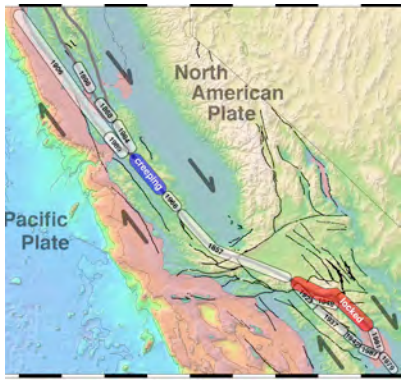

4-D Earthquake Cycle Model for Bounding Seismic Moment Accumulation Rate

David Sandwell
Xiaohua Xu
Bridget Smith-Konter
Xiaopeng Tong

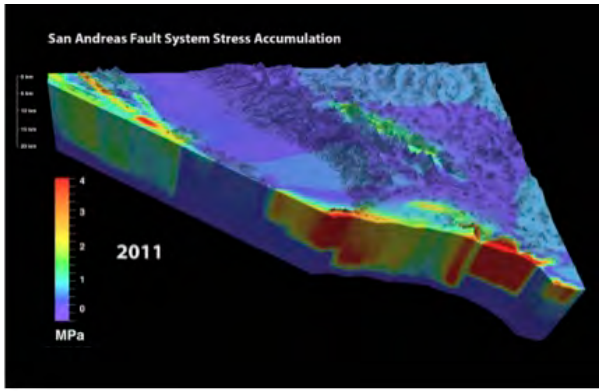

- What is the present-day seismic potential (moment) and stress along the main faults in the San Andreas system?
- Geodesy provides a direct measure of 2-D seismic moment accumulation rate.
- Semi-analytic 4-D viscoelastic earthquake cycle model developed using computer algebra.
- Estimate moment rate with geodesy, geology, paleo-seismology.
- What is missing?

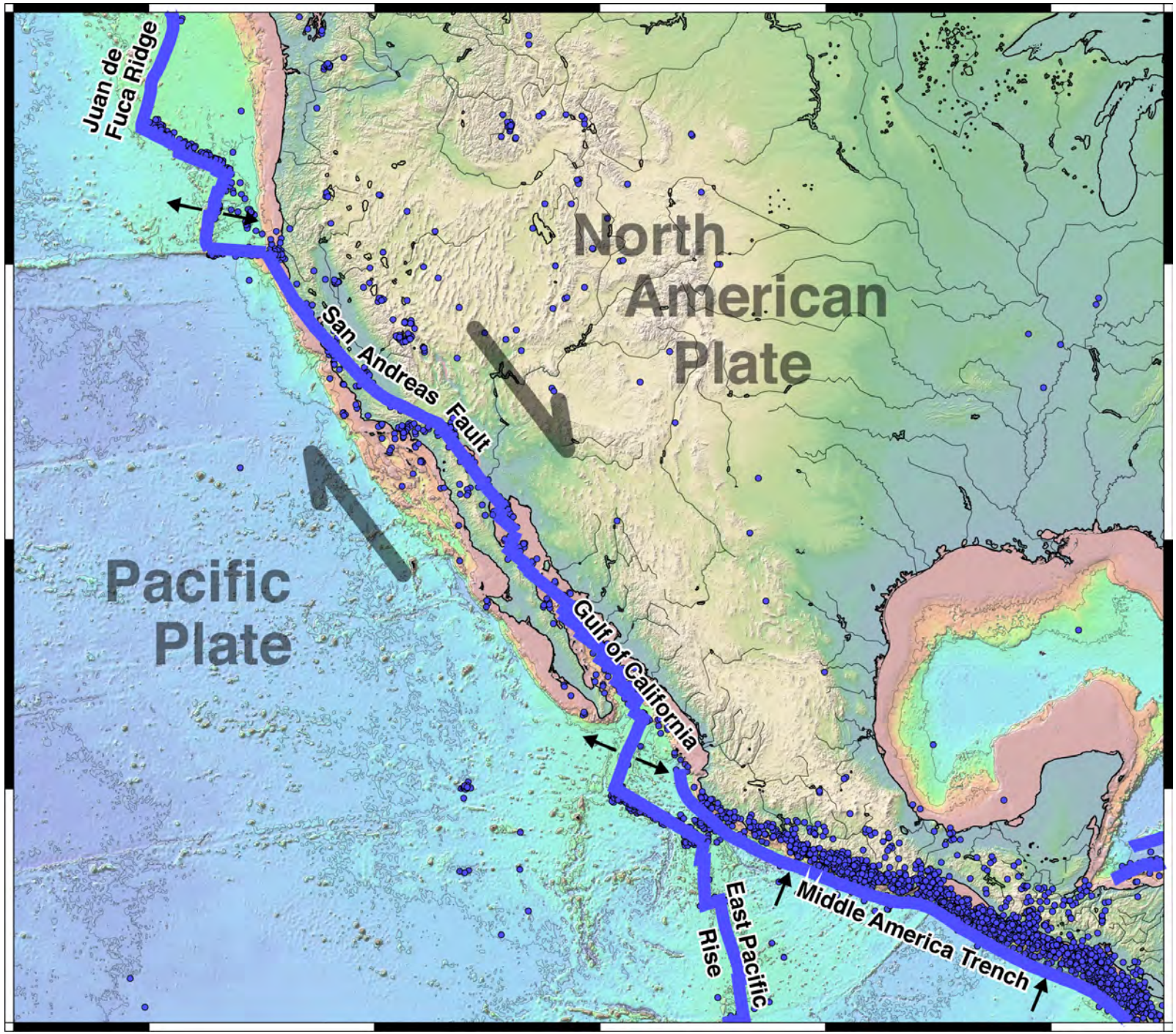
Juan de Fuca Ridge
North American Plate
San Andreas Fault
Pacific Plate
Gulf of California
East Pacific Rise
Middle America Trench

Earthquake Cycle

(modified from Tse and Rice, JGR, 1986)

100 to 10,000 yr

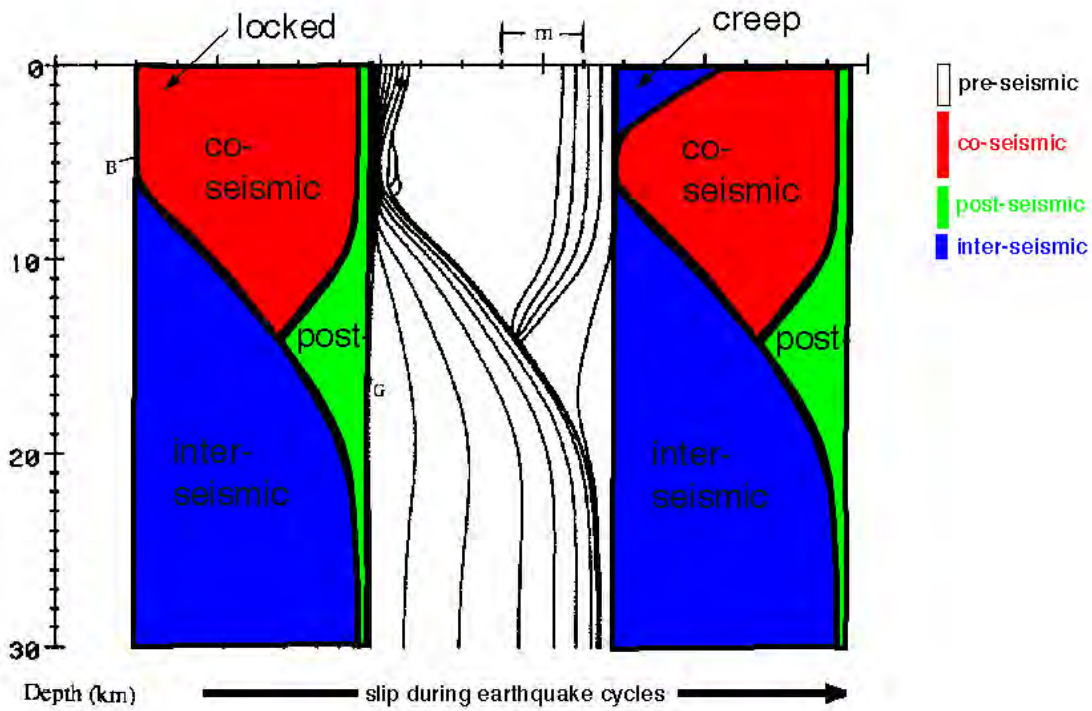

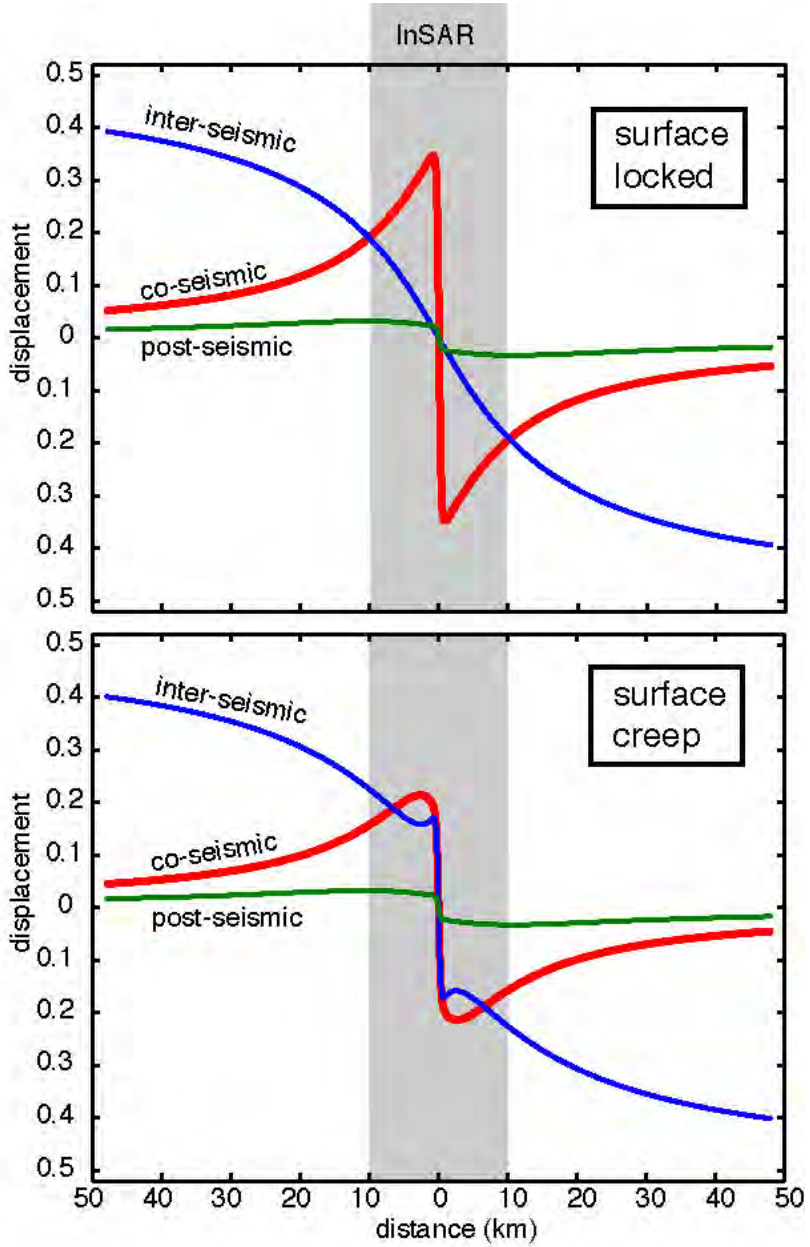

interseismic model

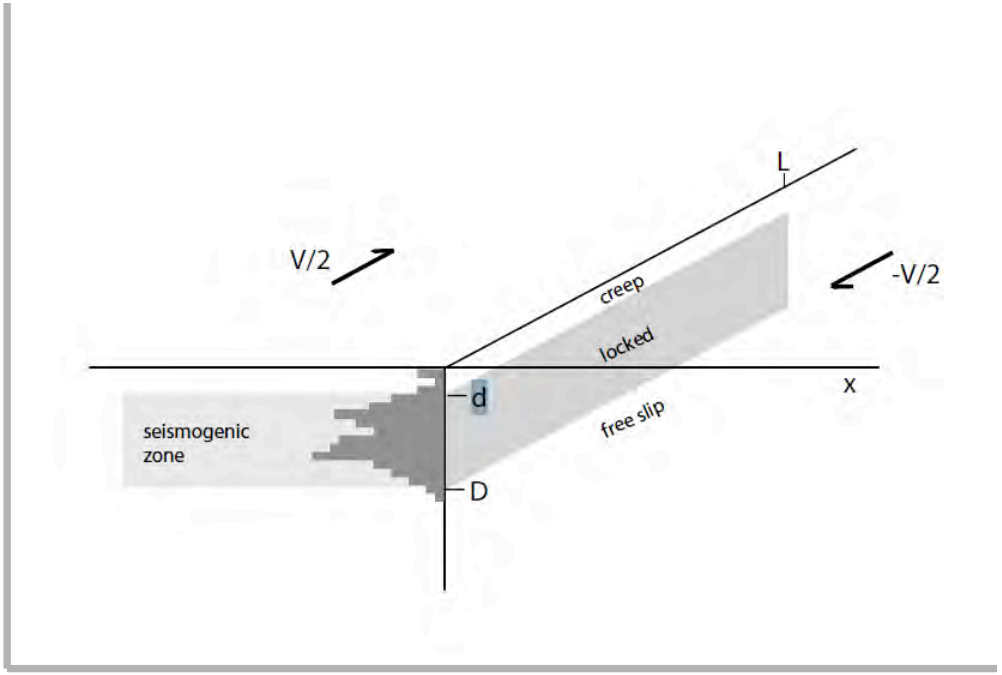

velocity $$v(x) = \frac{V}{\pi} \tan^{-1} \frac{x}{D}$$

strain rate $$\dot{\varepsilon}(x) = \frac{V}{\pi D} \frac{1}{1 + \left(\frac{x}{D}\right)^2} = \frac{\text{velocity}}{\text{depth}}$$

moment rate $$\frac{\dot{M}}{L} = \mu V D$$ = velocity X depth

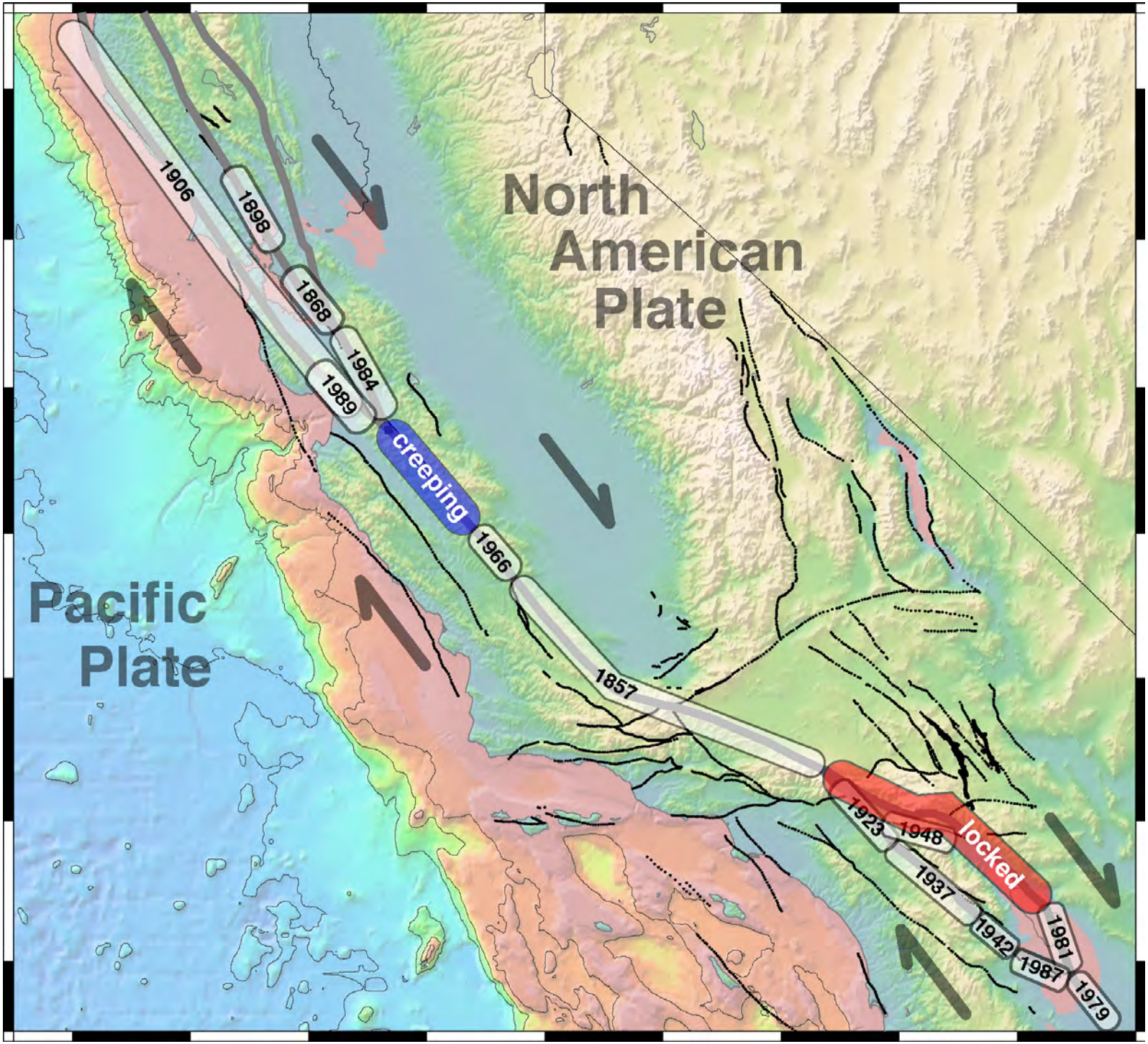
North American Plate
Pacific Plate
1906
1898
1868
1984
1989
creeping
1966
1857
1923
1948
locked
1937
1942
1981
1987
1979

seismic moment (2D)

interseismic moment accumulation rate

$$\frac{\dot{M}}{L} = \mu V D$$

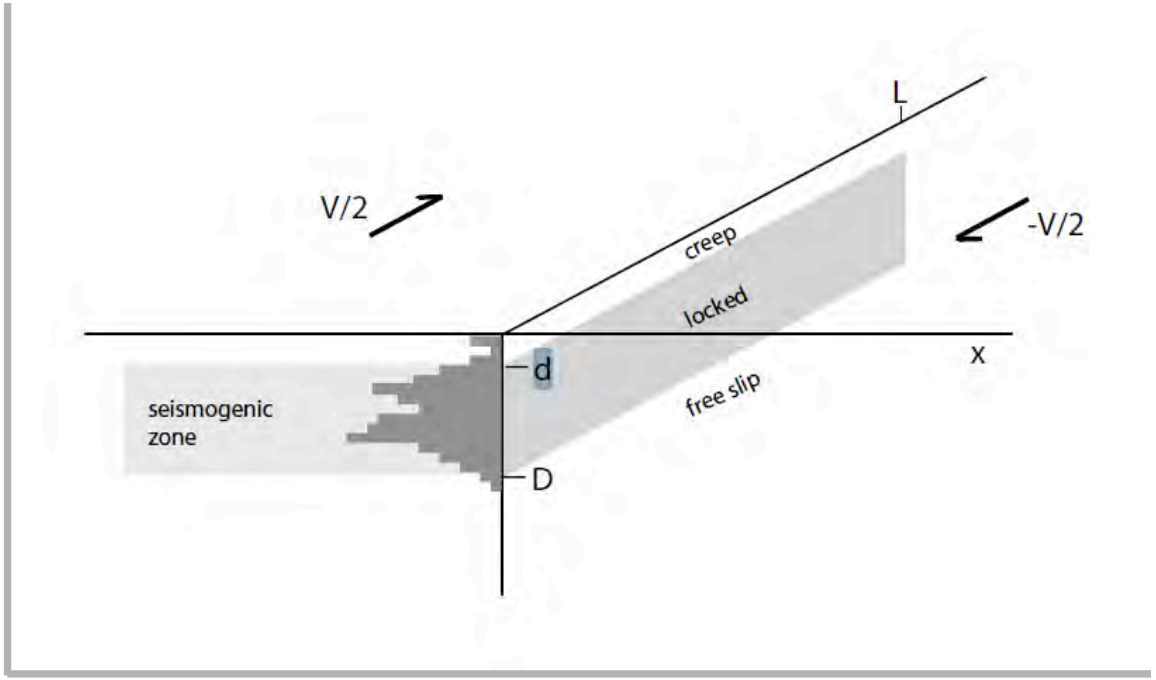

The size of the next earthquake depends on: the **slip rate** beneath the fault; times the **depth** of fault locking; times the **length** of the rupture; times the number of **years** since the last earthquake.

$$M = \mu V D L \, \Delta t$$

very different slip rate vs. depth have similar surface velocity and equal moment rate

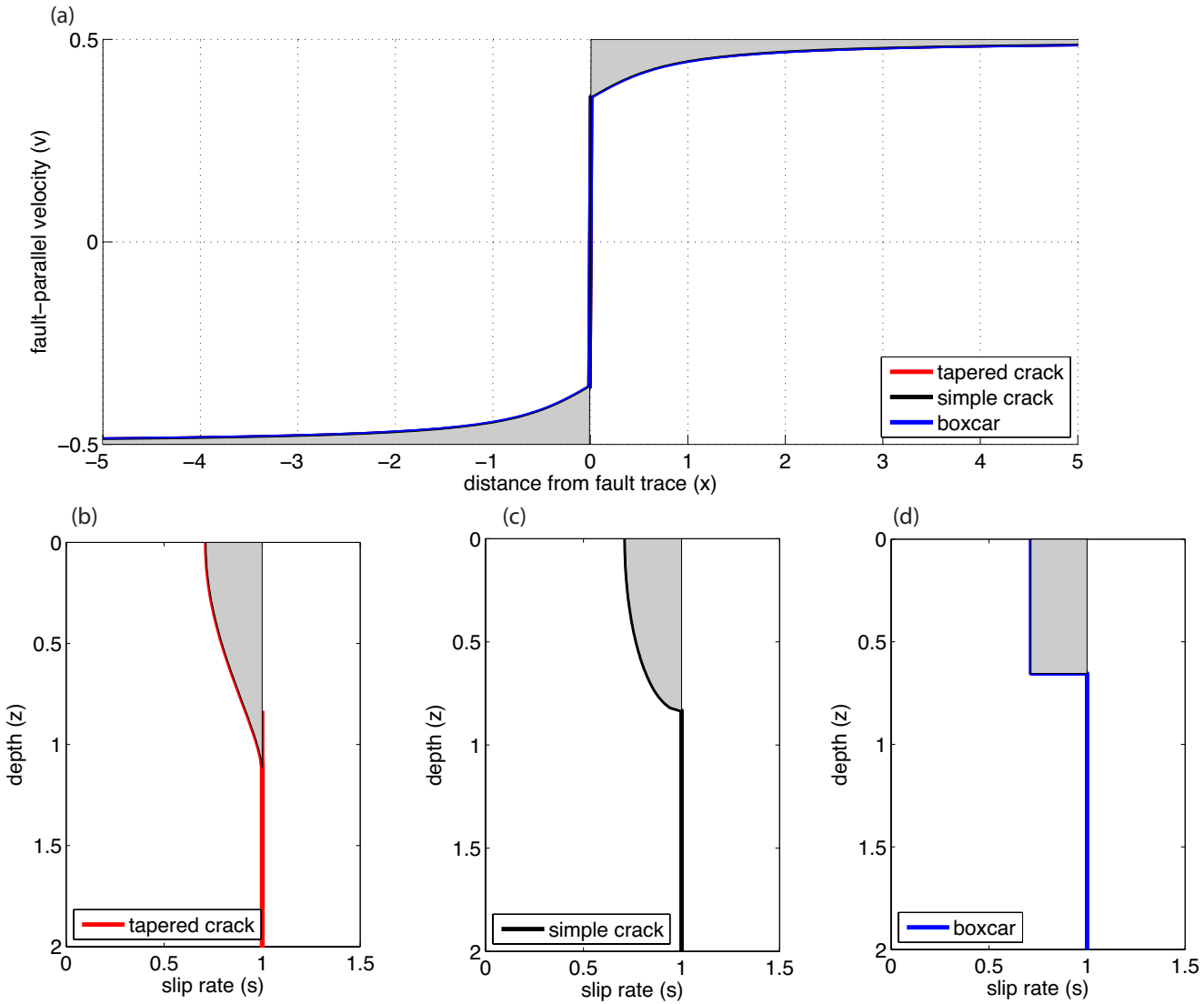

[Segall, 2010; Tong et al., 2015]

no inversion needed for moment rate

$$v(x) = \frac{1}{\pi} \int_{-D_m}^{0} \frac{s(z)x}{x^2 + z^2} dz$$

$$\frac{M}{L} = \mu \int_{-D_m}^{0} s(z) dz$$

exercise - show that

$$\frac{M}{L} = \lim_{W \to \infty} \frac{\mu\pi}{2W} \int_{-W}^{W} x v(x) dx, \qquad W >> D_m$$

can be measured

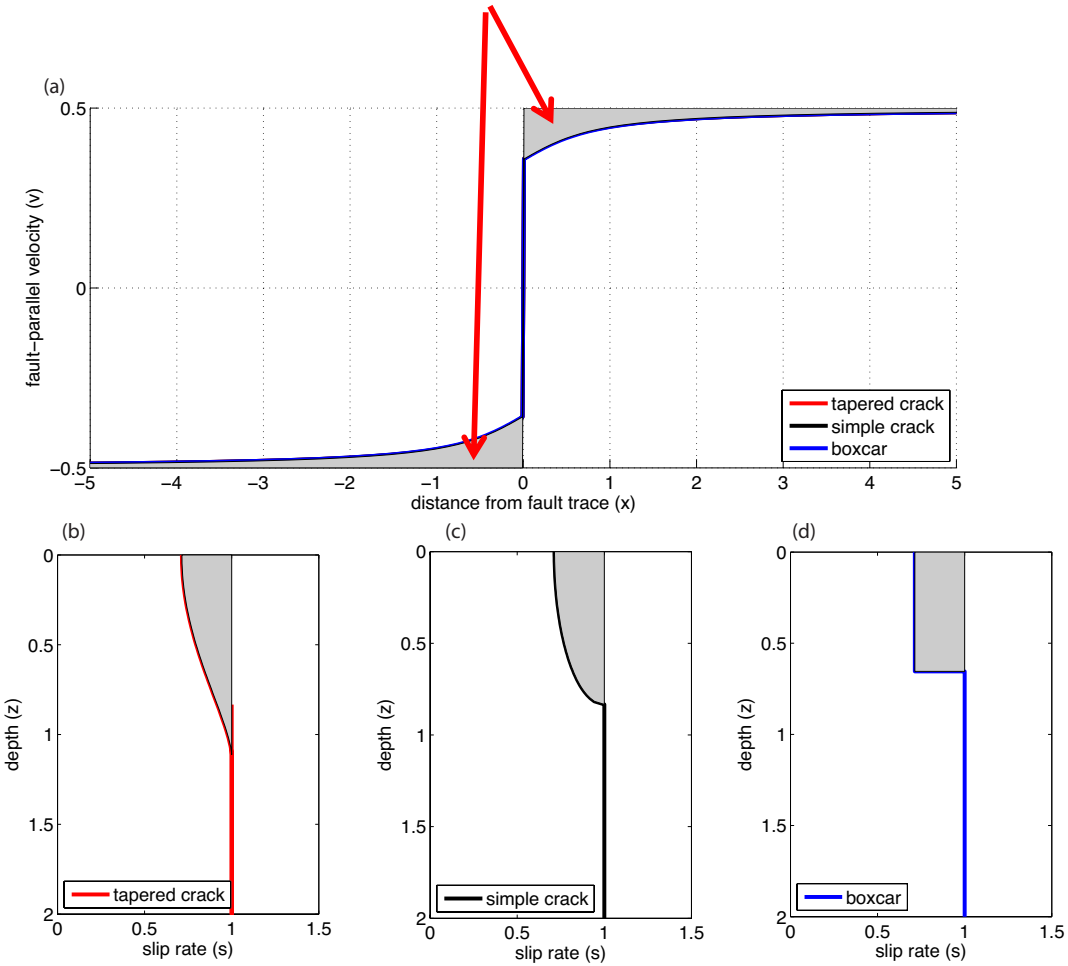

difference between block model and interseismic model

need both high accuracy and small-scale (< 20 km) resolution
to measure moment rate

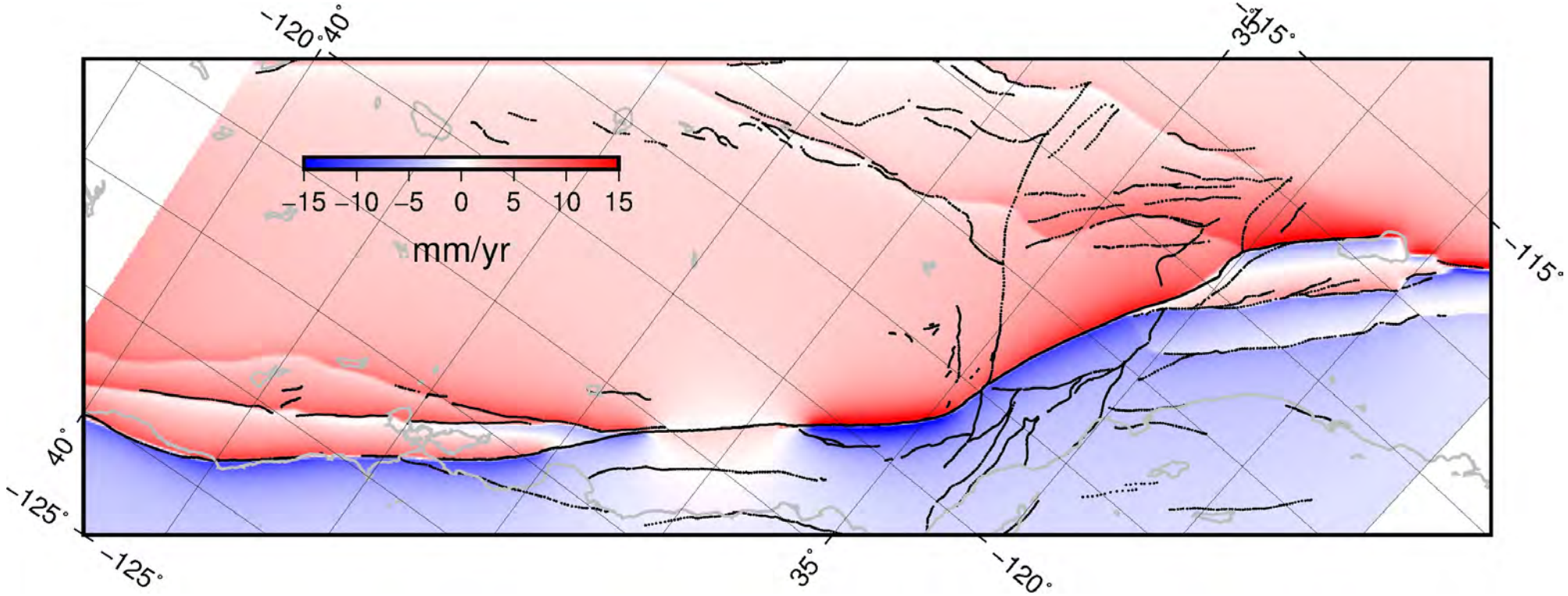

The approach invert for both slip rate and locking depth on all the faults and establish bounds on the moment rate [Johnson et al., 2014; Tong et al., 2015]. This assumes we have identified all the faults.

Average of 10 velocity models based on the same GPS vectors – CGM V1.0

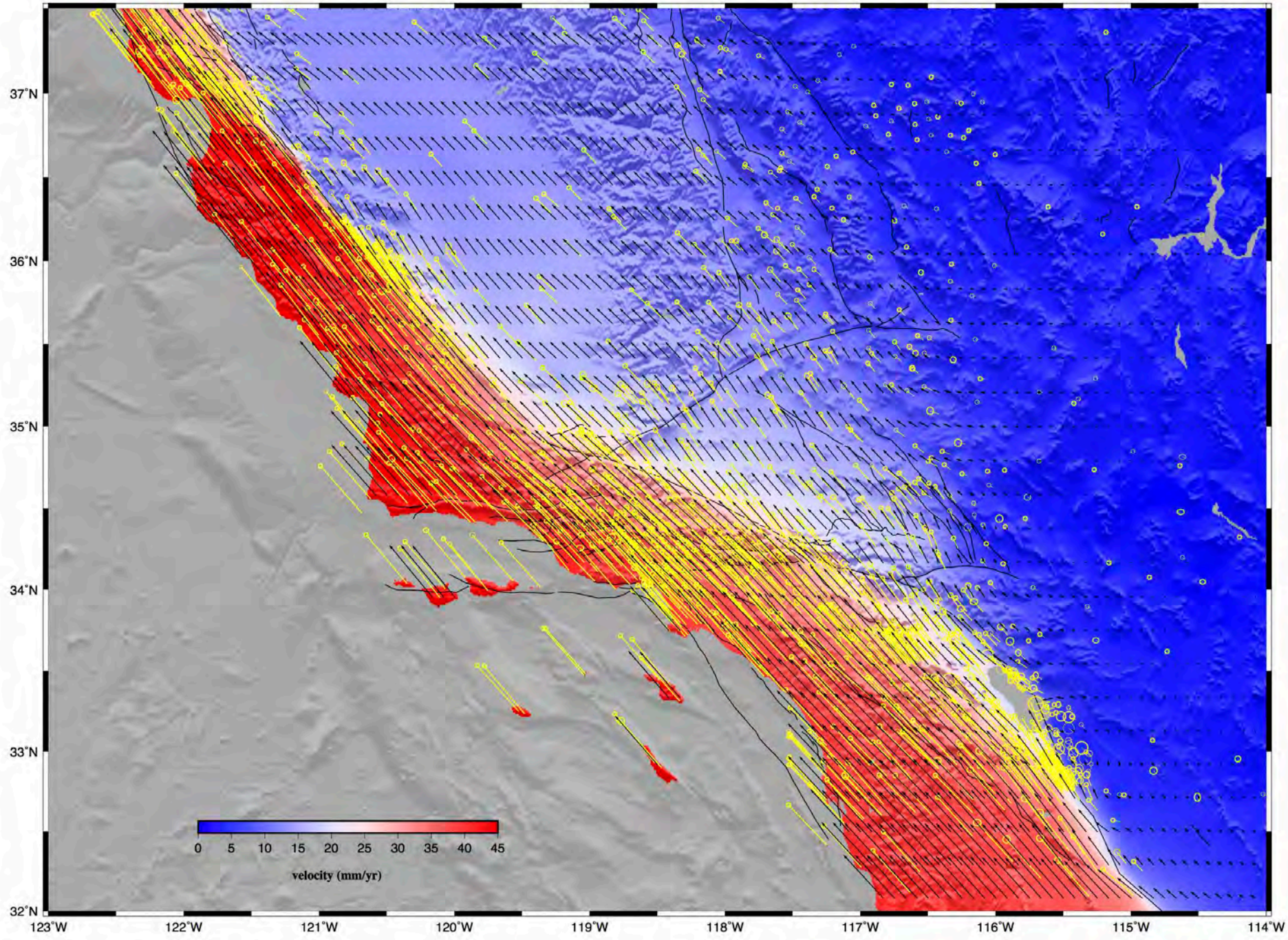

Standard deviation of 10 velocity models based on the same GPS vectors – CGM V1.0

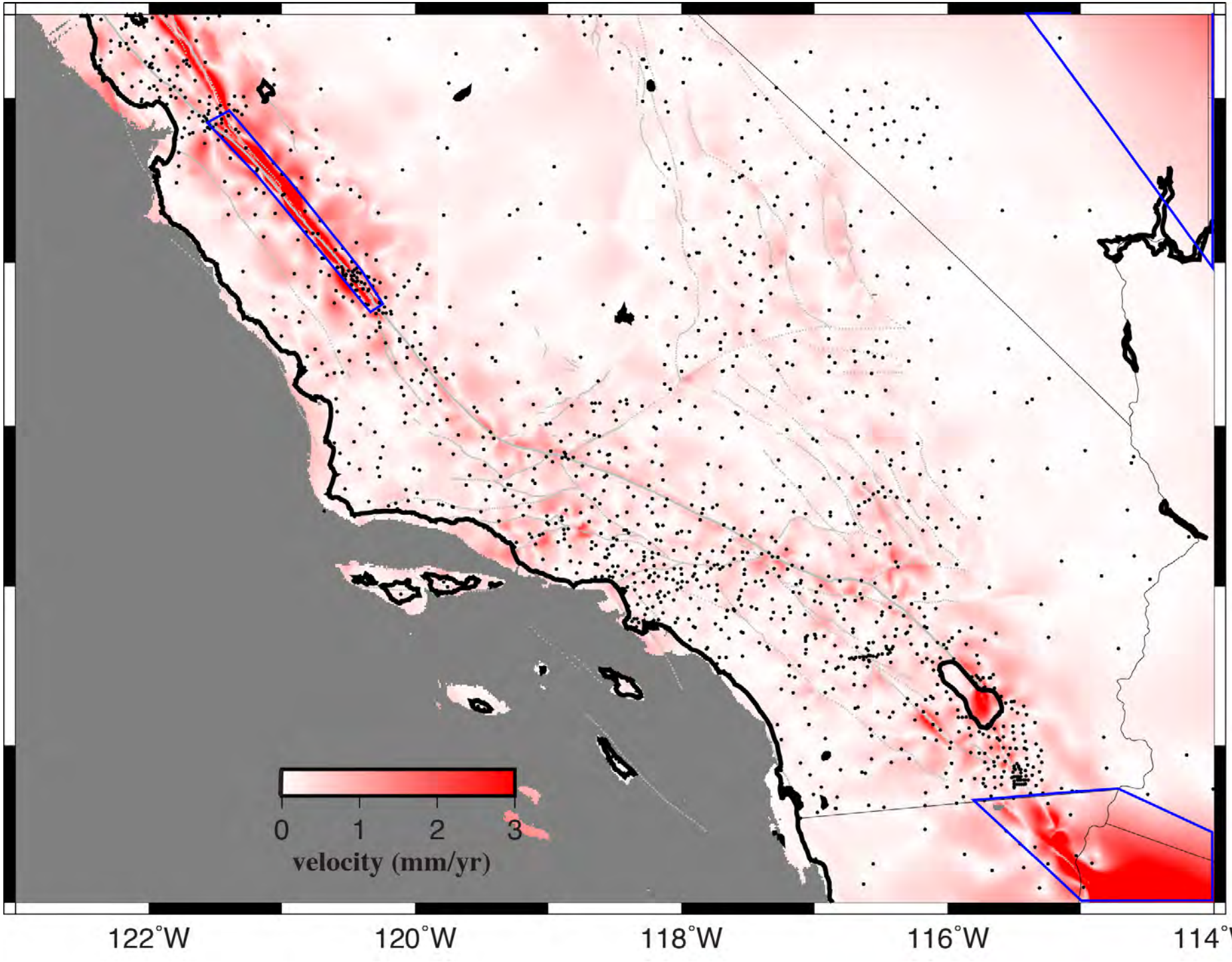

median spacing of GPS stations

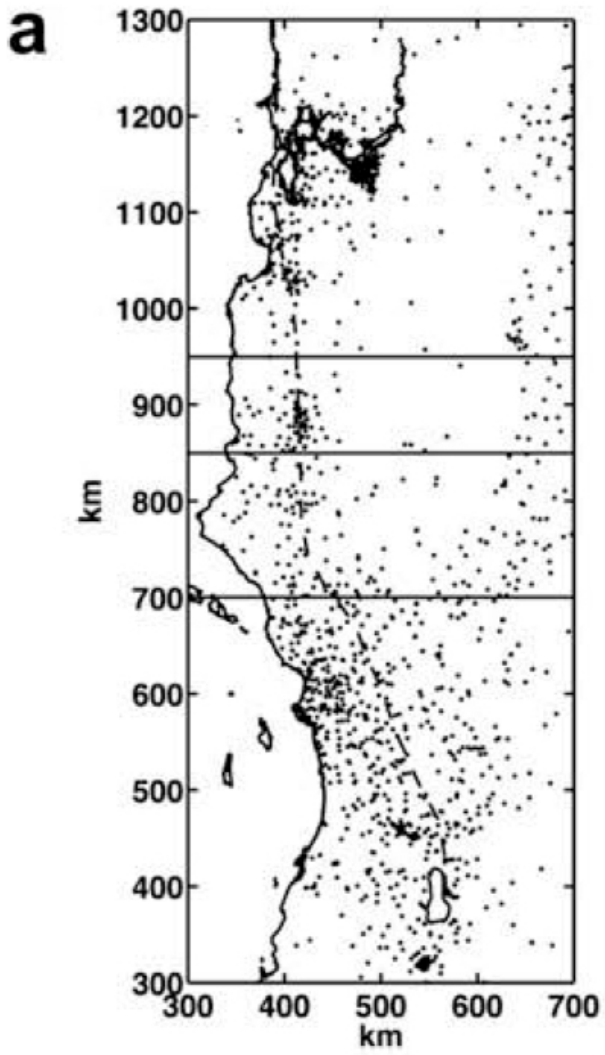

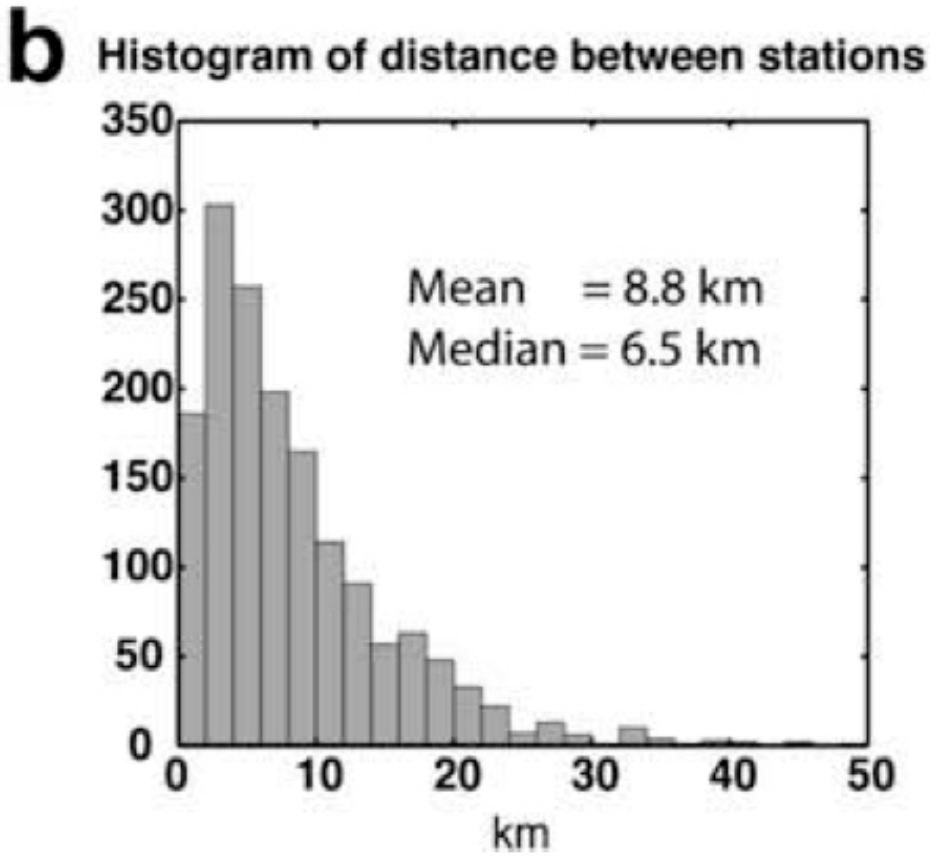

[Wei et al. 2010]

InSAR/GPS Integration Approach

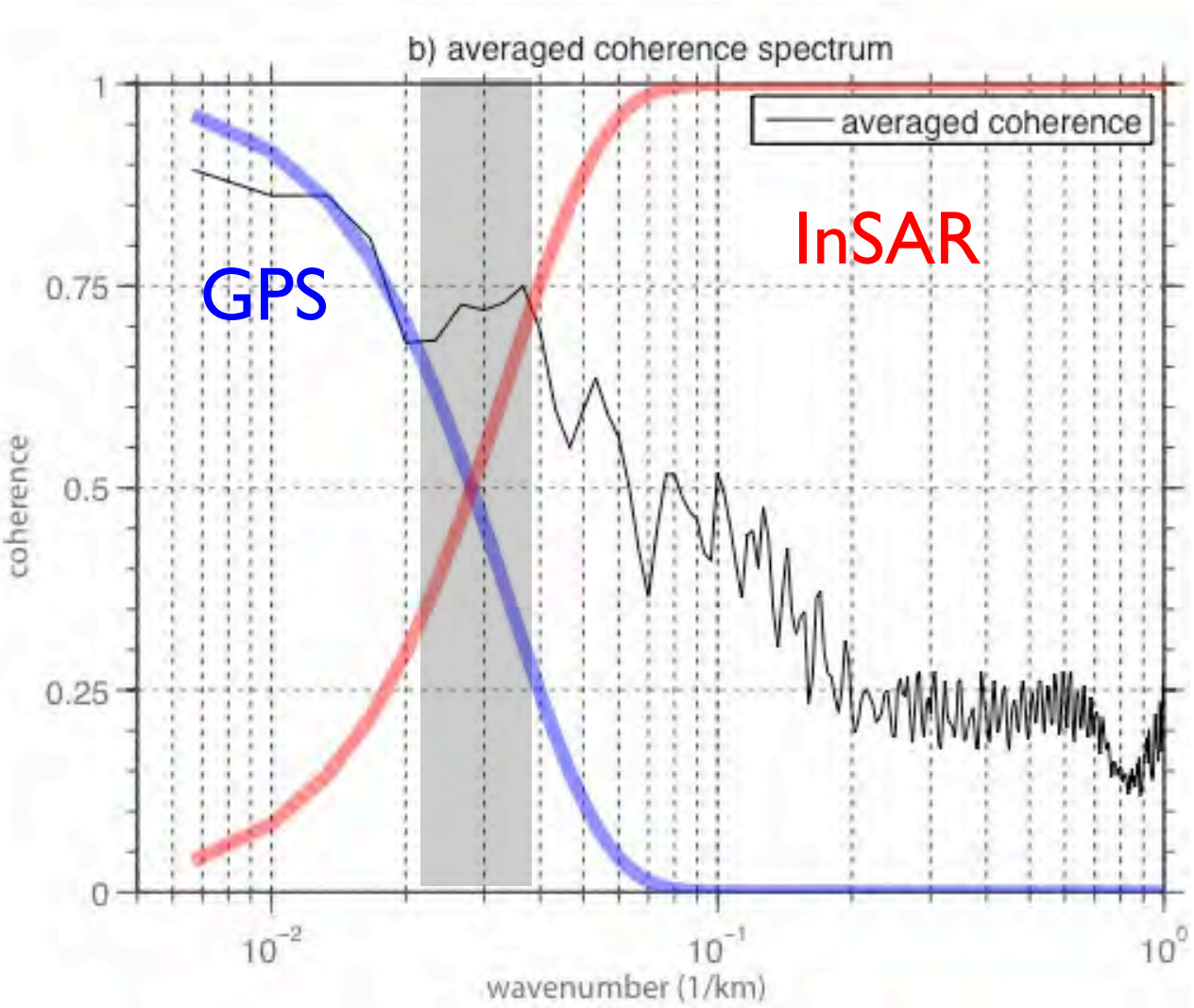

1. Develop a complete surface velocity field based on a kinematic model constrained by GPS secular velocity data.
2. Refine the kinematic model using biharmonic spline correction from GPS misfits.
3. Stack InSAR interferograms to derive an InSAR secular velocity.
4. Remove the GPS model from the InSAR velocity
5. High-pass filter the InSAR residual velocity.
6. Restore the GPS model to the InSAR residual velocity.

[Tong et al., 2013]

Sentinel-1 Results

- The San Andreas
  - Sentinel-1 data for California 2015.3 – 2019.3
  - 5 descending tracks of 20 bursts long; 37-62 repeats

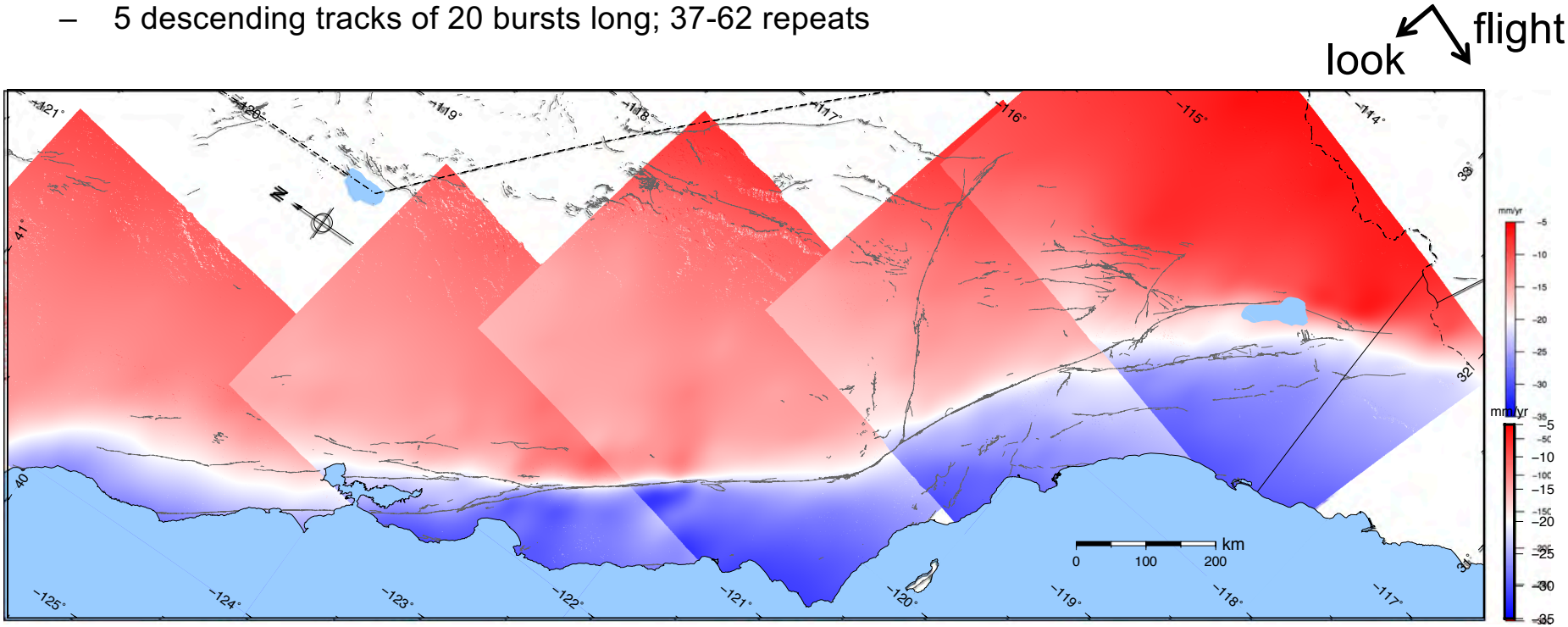

LOS velocity map

Xu and Sandwell, in prep

Sentinel-1/GPS

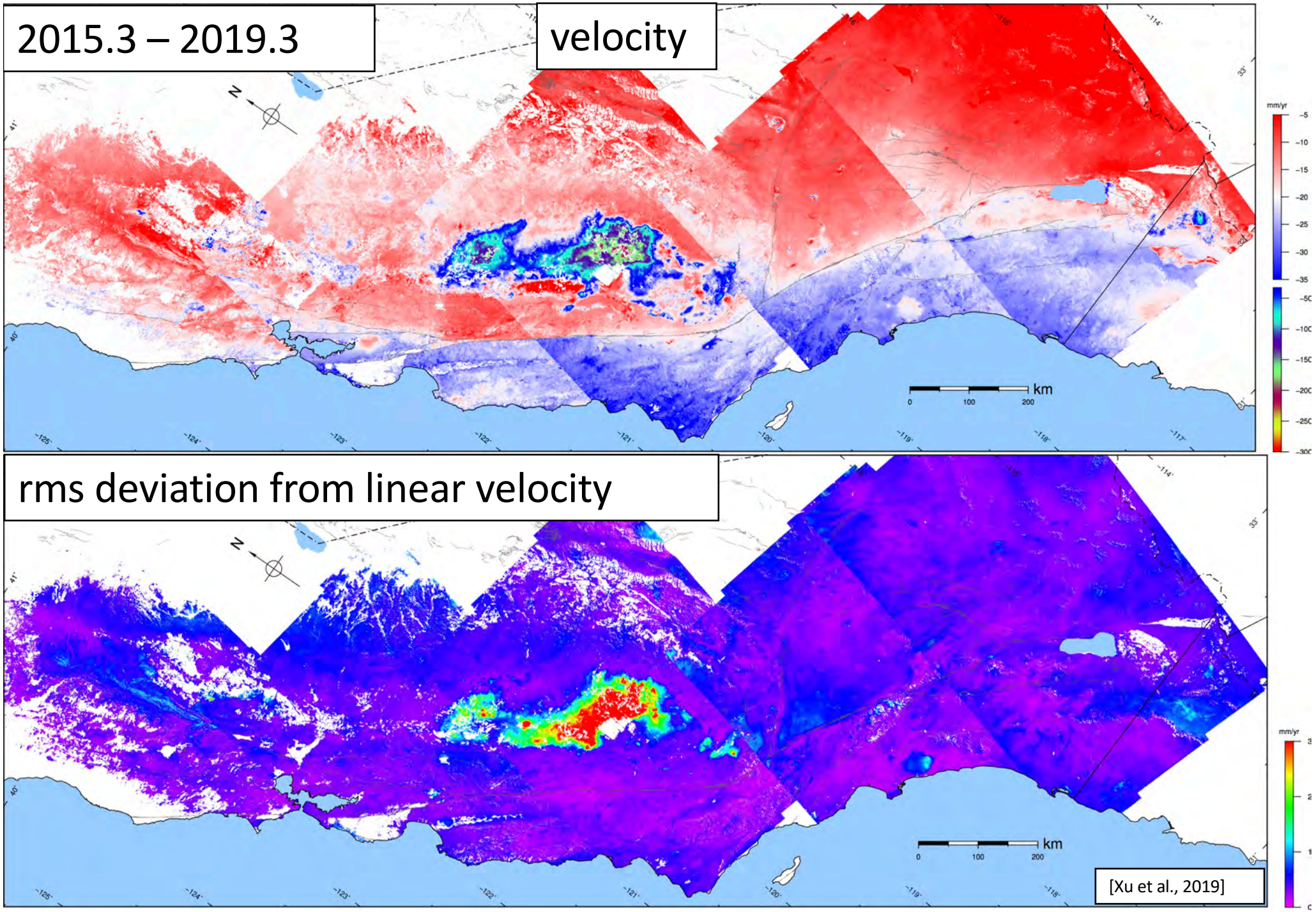

Sentinel-1 Expectations

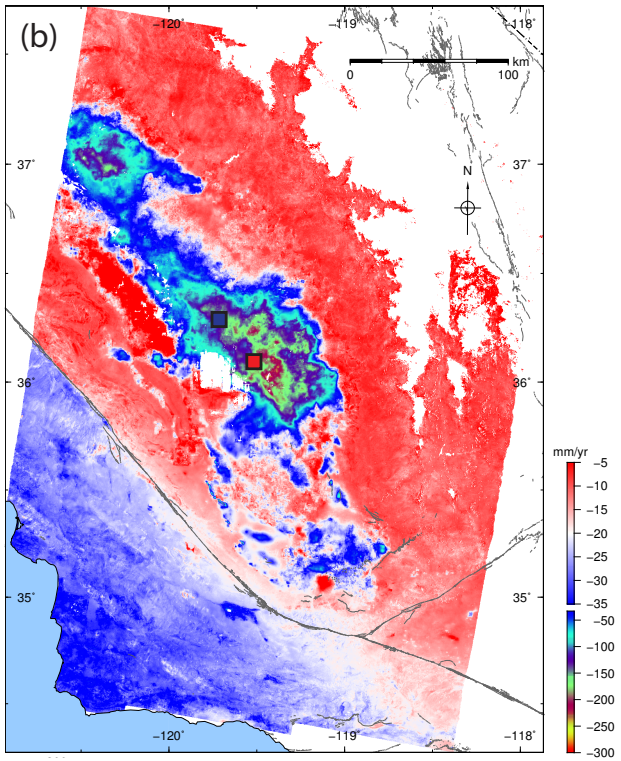

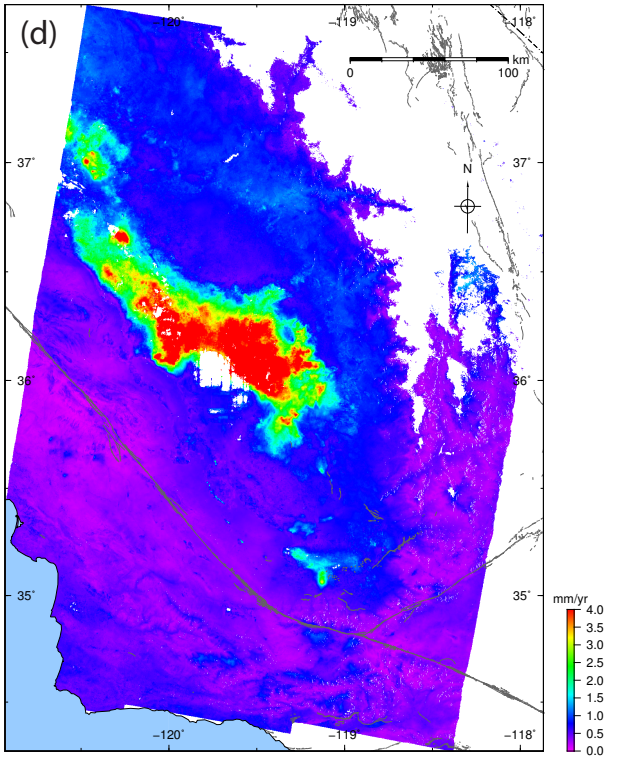

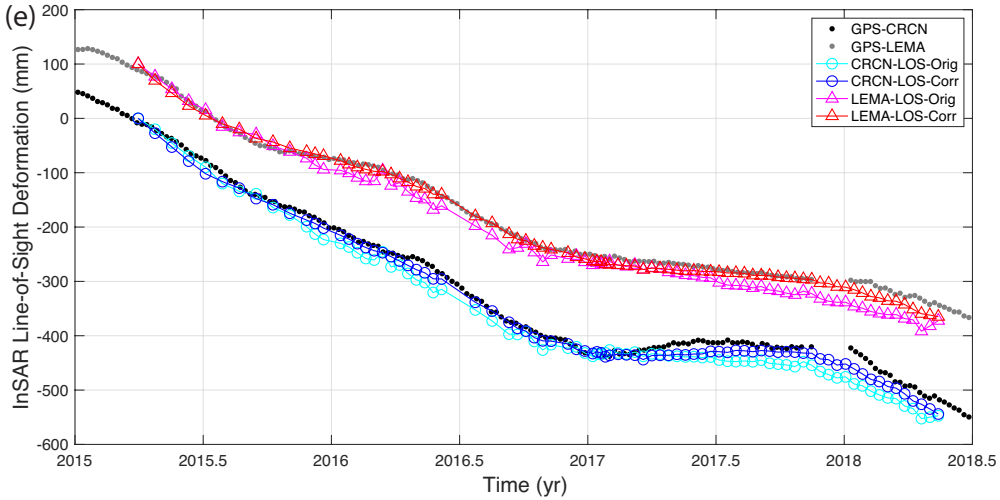

Emardson et al. 2003

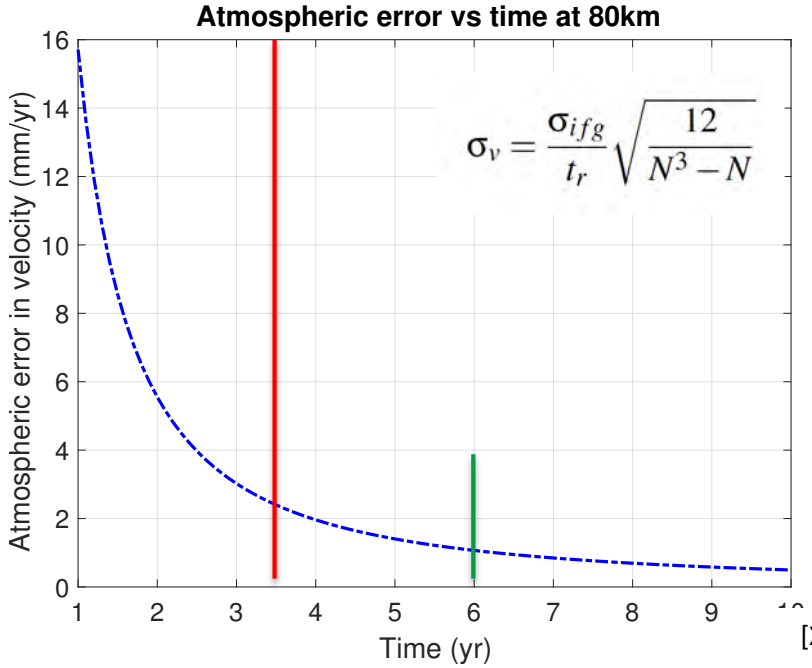

[Xu et al., 2019]

4-D earthquake cycle models

	elastic block model	viscoelastic plate model	numerical model
pro	simple Green's function fast	time-dependent fast stress and strain are continuous	non-linear rheology existing codes
con	no time-dependent rheology stress singularities at fault intersections inaccurate vertical displacements	complicated algebra linear rheology only	complicated numerical codes difficult setup/meshing too slow for exhaustive parameter search

force couples in elastic plate over viscoelastic half space

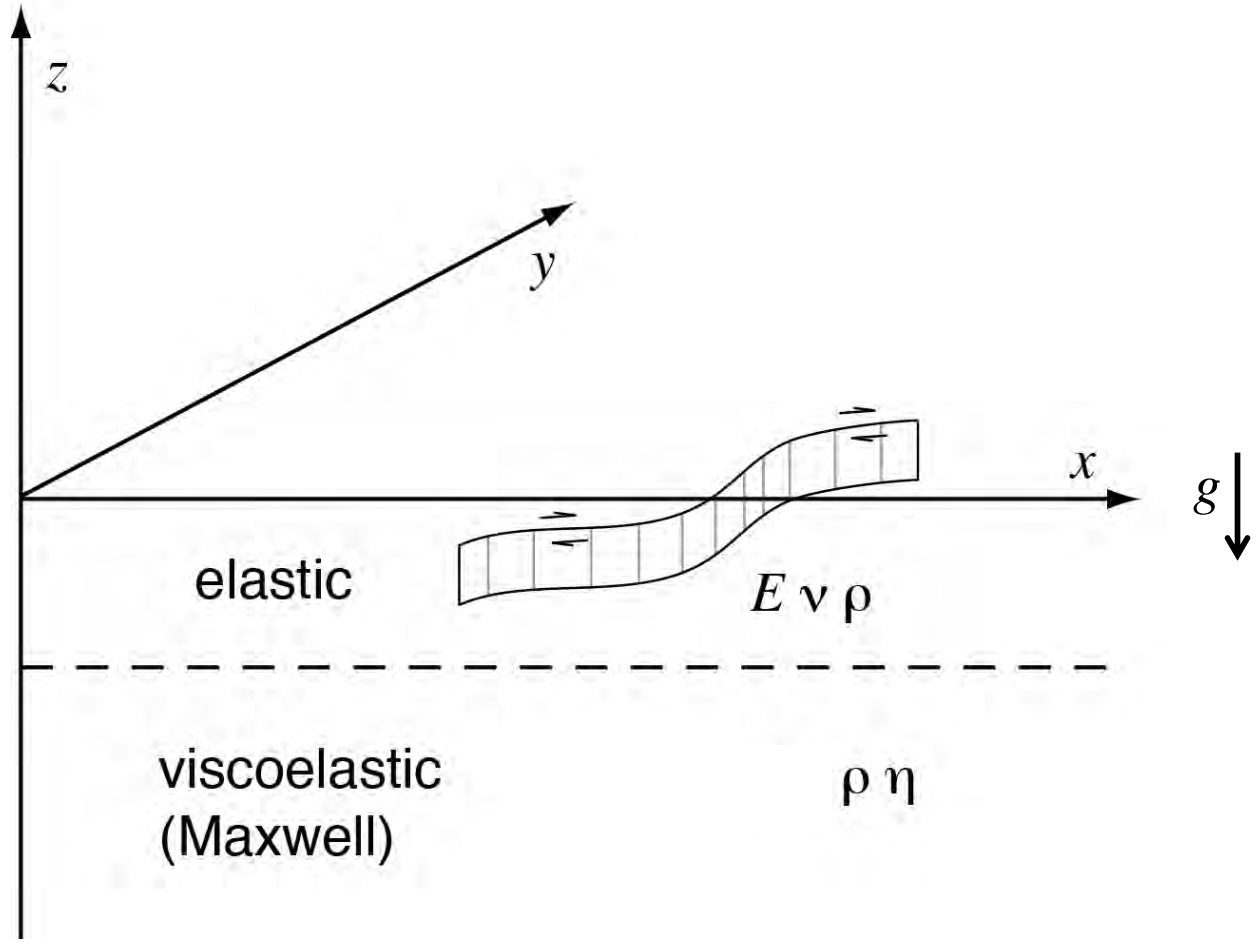

outline of solution for vertical strike-slip fault

[*Smith-Konter and Sandwell*, 2004]

0) do all calculations in horizontal Fourier transform space (k_x, k_y, z)

1) solve for response of elastic full space to vector body force and integrate over fault depth

2) use method of images to simulate a layer over a half space [*Rybicki*, 1971].

3) match zero traction surface boundary condition using Galerkin vector approach [*Steketee*, 1958]

4) modify the *Steketee* [1958] approach to solve for layer over half space - **NEW**

5) use the elastic-viscoelastic correspondence principle to map half-space viscoelastic parameters to elastic parameters

6) create grids of double-couple forces to simulate faults [*Burridge and Knopoff*, 1964]

NEW

Boussinesq problem for point load on layer over half space with gravity restoring force

---

$\tau_{zz1} = -\tau_{33} + \rho g W_1\big|_{z=0}$ $\qquad$ $\tau_{xz1} = \tau_{yz1} = 0\big|_{z=0}$ $\qquad$ surface boundary conditions (2 – radial symmetry)

$\tau_{xz1} = \tau_{xz2}\big|_{z=-h}$ $\qquad$ $U_1 = U_2\big|_{z=-h}$

$\tau_{yz1} = \tau_{yz2}\big|_{z=-h}$ $\qquad$ $V_1 = V_2\big|_{z=-h}$

$\tau_{zz1} = \tau_{zz2}\big|_{z=-h}$ $\qquad$ $W_1 = W_2\big|_{z=-h}$

continuous displacement and
stress at base of layer (4 – radial symmetry)

Need to invert this 6X6 algebraic system analytically. – GOOD LUCK!!!!

$$\begin{bmatrix} 1 \\ 0 \\ 0 \\ 0 \\ 0 \\ 0 \end{bmatrix} = \begin{bmatrix} \chi\beta(2\mu_1\beta-\rho g) & \chi\beta(2\mu_1\beta+\rho g) & 2\chi(\mu_1\beta(3-1/\eta_1)-\rho g(1-1/\alpha_1)) & -2\chi(\mu_1\beta(3-1/\eta_1)+\rho g(1-1/\alpha_1)) & 0 & 0 \\ \beta & -\beta & (2-1/\alpha_1) & (2-1/\alpha_1) & 0 & 0 \\ \mu_1\alpha_1\beta e^{-\beta h} & -\mu_1\alpha_1\beta e^{\beta h} & \mu_1\alpha_1(2-\beta h-1/\alpha_1)e^{-\beta h} & \mu_1\alpha_1(2+\beta h-1/\alpha_1)e^{\beta h} & -\mu_2\alpha_2\beta e^{-\beta h} & -\mu_2\alpha_2(2-\beta h-1/\alpha_2)e^{-\beta h} \\ \mu_1\alpha_1\beta e^{-\beta h} & \mu_1\alpha_1\beta e^{\beta h} & \mu_1\alpha_1(3-\beta h-1/\eta_1)e^{-\beta h} & -\mu_1\alpha_1(3+\beta h-1/\eta_1)e^{\beta h} & -\mu_2\alpha_2\beta e^{-\beta h} & -\mu_2\alpha_2(3-\beta h-1/\eta_2)e^{-\beta h} \\ \alpha_1\beta e^{-\beta h} & \alpha_1\beta e^{\beta h} & \alpha_1(1-\beta h)e^{-\beta h} & -\alpha_1(1+\beta h)e^{\beta h} & -\alpha_2\beta e^{-\beta h} & -\alpha_2(1-\beta h)e^{-\beta h} \\ \alpha_1\beta e^{-\beta h} & -\alpha_1\beta e^{\beta h} & \alpha_1(2-\beta h-2/\alpha_1)e^{-\beta h} & \alpha_1(2+\beta h-2/\alpha_1)e^{\beta h} & -\alpha_2\beta e^{-\beta h} & -\alpha_2(2-\beta h-2/\alpha_2)e^{-\beta h} \end{bmatrix} \begin{bmatrix} A_1 \\ B_1 \\ C_1 \\ D_1 \\ A_2 \\ C_2 \end{bmatrix}$$

$$\begin{bmatrix} 1 \\ 0 \\ 0 \\ 0 \\ 0 \\ 0 \end{bmatrix} = \begin{bmatrix} \chi\beta(2\mu_1\beta-\rho g) & \chi\beta(2\mu_1\beta+\rho g) & 2\chi\left(\mu_1\beta(3-1/\eta_1)-\rho g(1-1/\alpha_1)\right) & -2\chi\left(\mu_1\beta(3-1/\eta_1)+\rho g(1-1/\alpha_1)\right) & 0 & 0 \\ \beta & -\beta & (2-1/\alpha_1) & (2-1/\alpha_1) & 0 & 0 \\ \mu_1\alpha_1\beta e^{-\beta h} & -\mu_1\alpha_1\beta e^{\beta h} & \mu_1\alpha_1(2-\beta h-1/\alpha_1)e^{-\beta h} & \mu_1\alpha_1(2+\beta h-1/\alpha_1)e^{\beta h} & -\mu_2\alpha_2\beta e^{-\beta h} & -\mu_2\alpha_2(2-\beta h-1/\alpha_2)e^{-\beta h} \\ \mu_1\alpha_1\beta e^{-\beta h} & \mu_1\alpha_1\beta e^{\beta h} & \mu_1\alpha_1(3-\beta h-1/\eta_1)e^{-\beta h} & -\mu_1\alpha_1(3+\beta h-1/\eta_1)e^{\beta h} & -\mu_2\alpha_2\beta e^{-\beta h} & -\mu_2\alpha_2(3-\beta h-1/\eta_2)e^{-\beta h} \\ \alpha_1\beta e^{-\beta h} & \alpha_1\beta e^{\beta h} & \alpha_1(1-\beta h)e^{-\beta h} & -\alpha_1(1+\beta h)e^{\beta h} & -\alpha_2\beta e^{-\beta h} & -\alpha_2(1-\beta h)e^{-\beta h} \\ \alpha_1\beta e^{-\beta h} & -\alpha_1\beta e^{\beta h} & \alpha_1(2-\beta h-2/\alpha_1)e^{-\beta h} & \alpha_1(2+\beta h-2/\alpha_1)e^{\beta h} & -\alpha_2\beta e^{-\beta h} & -\alpha_2(2-\beta h-2/\alpha_2)e^{-\beta h} \end{bmatrix} \begin{bmatrix} A_1 \\ B_1 \\ C_1 \\ D_1 \\ A_2 \\ C_2 \end{bmatrix}$$

Today we have symbolic algebra – no sweat, no errors!!

```
% set up left hand side

Y=[1; 0; 0; 0; 0; 0;];

% set up right hand side

M=[ X*m*(2*u1*m-p*g)  X*m*(2*u1*m+p*g)  2*X*( u1*m*(3-ie1) -p*g*(1-ia1) )   -2*X*( u1*m*(3-ie1) + p*g*(1-ia1) )   0    0;
   m       -m       (2-ia1)            (2-ia1)          0        0;
   ma1*m*en  -ma1*m*ep  ma1*(2-mh-ia1)*en     ma1*(2+mh-ia1)*ep  -ma2*m*en  -ma2*(2-mh-ia2)*en;
   ma1*m*en   ma1*m*ep  ma1*(3-mh-ie1)*en    -ma1*(3+mh-ie1)*ep  -ma2*m*en  -ma2*(3-mh-ie2)*en;
   a1*m*en   a1*m*ep  a1*(1-mh)*en        -a1*(1+mh)*ep      -a2*m*en   -a2*(1-mh)*en;
   a1*m*en   -a1*m*ep  a1*(2-mh-(2*ia1))*en  a1*(2+mh-2*ia1)*ep -a2*m*en   -a2*(2-mh-(2*ia2))*en];

% invert matrix

Z=M\Y;
```

tests with half-space [*Love,* 1944] and thin-plate flexure

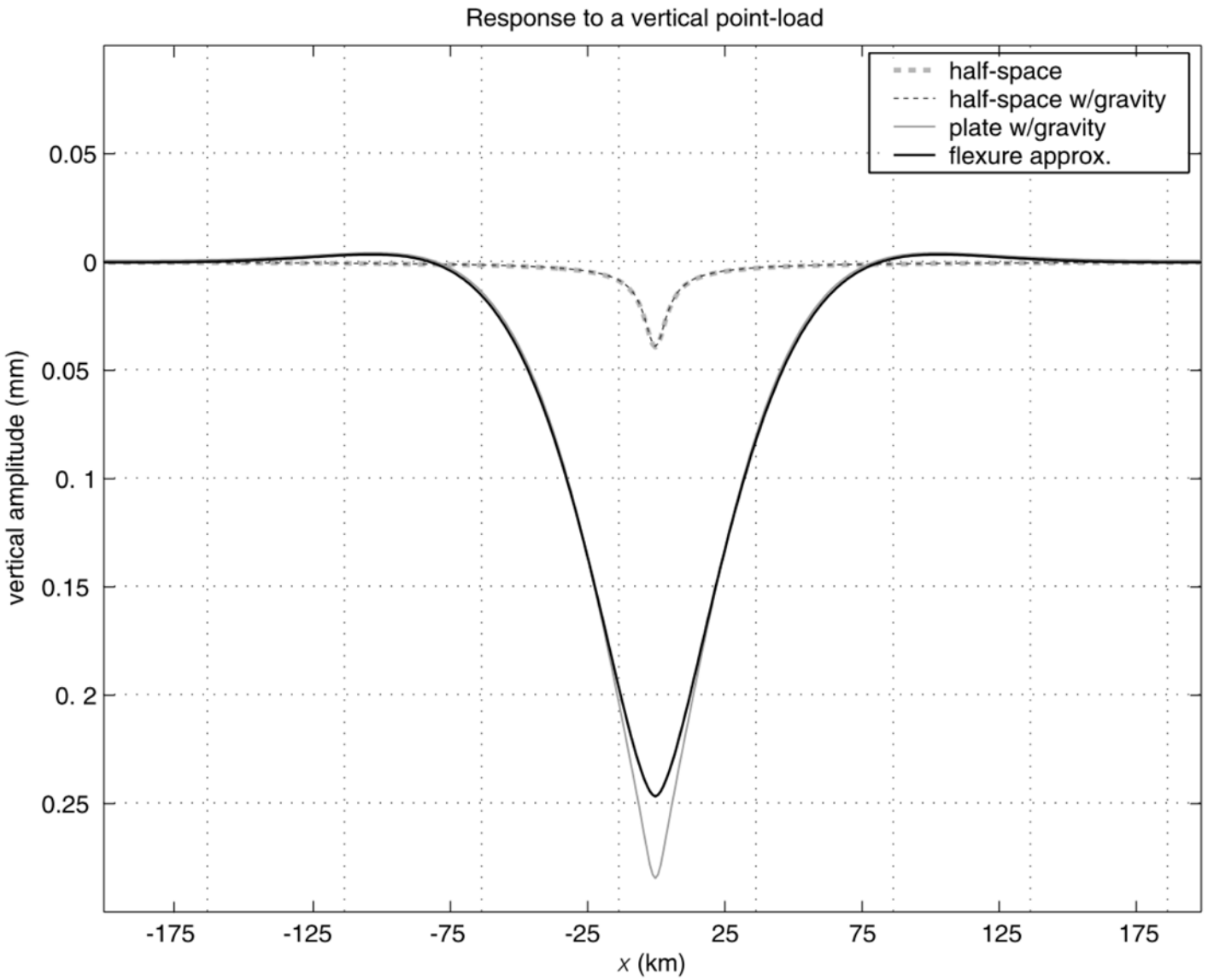

gravity dominates for plate model but is unimportant for half space model.

spinning plate benchmark

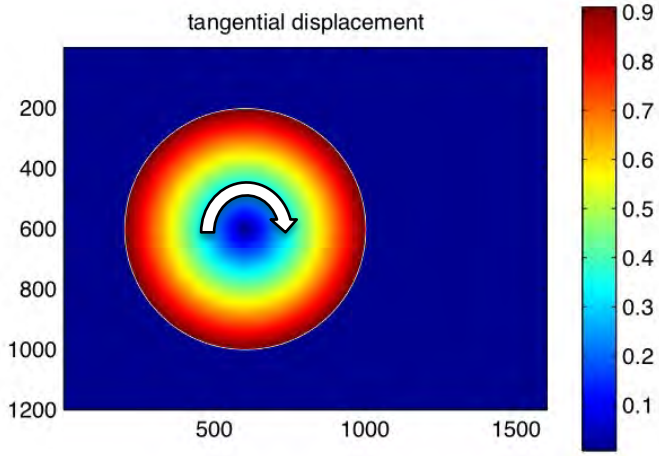

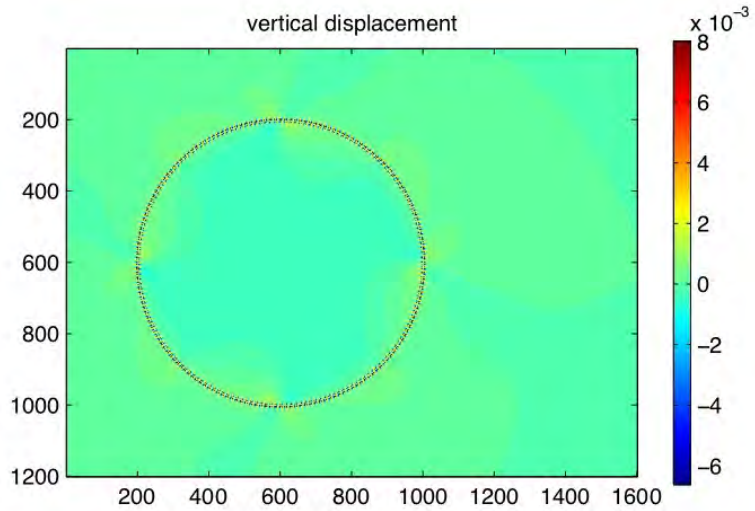

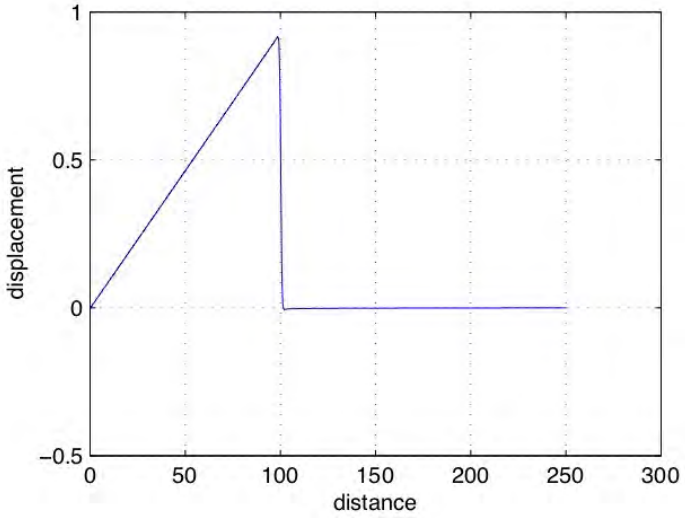

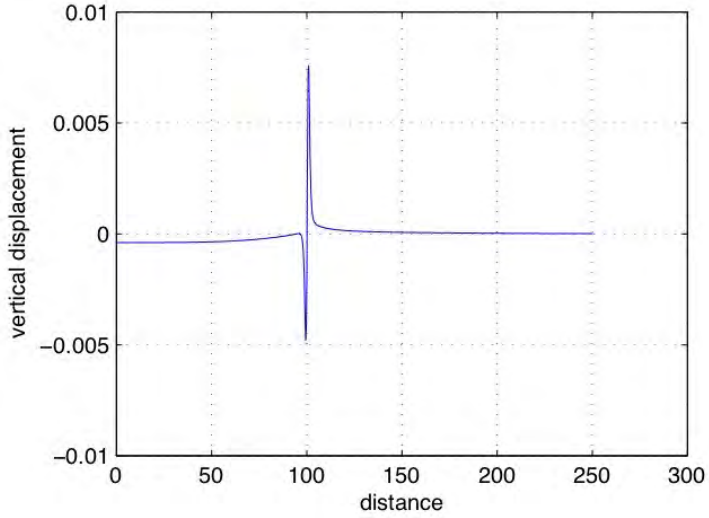

Don’t need fake blocks with backslip but can have true plate-like behavior that couples far-field velocity to near-fault stress.

need thick plate and gravity to simulate vertical deformation

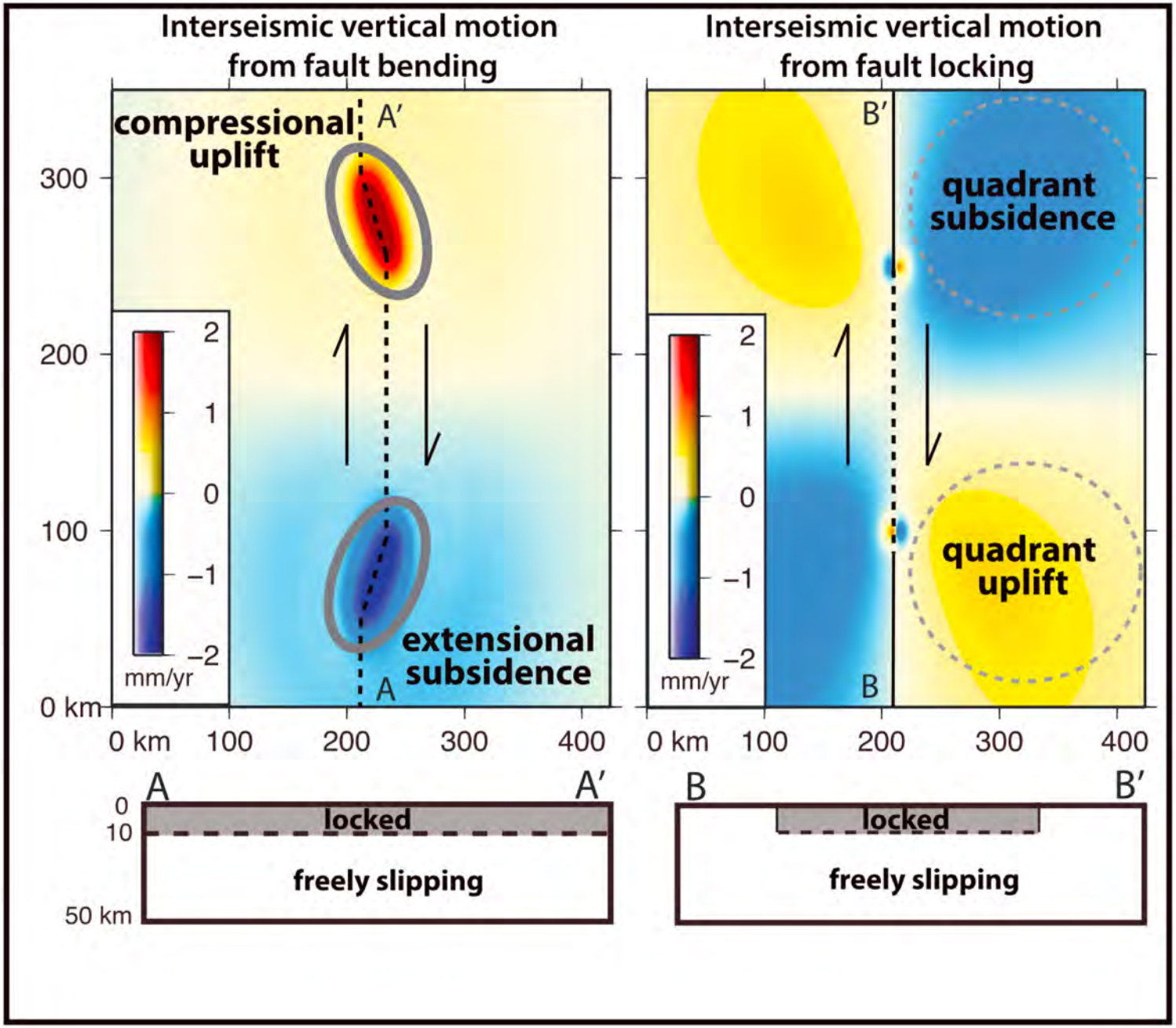

Kinematic Earthquake Cycle Model

[Smith and Sandwell, JGR, 2006]

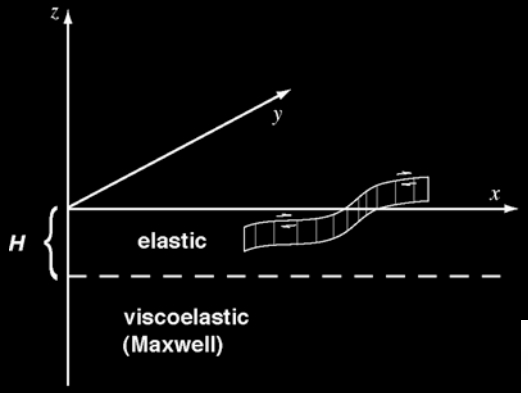

Simple model

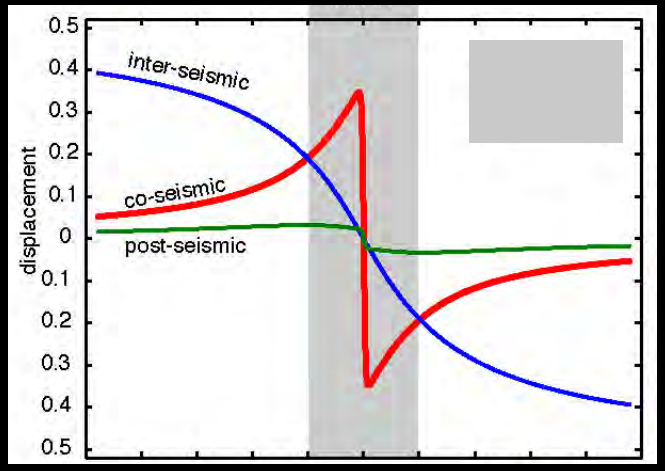

[Tse and Rice, JGR, 1986]

displacement(t) =

interseismic + Σ earthquakes

(deep slip) (shallow slip)

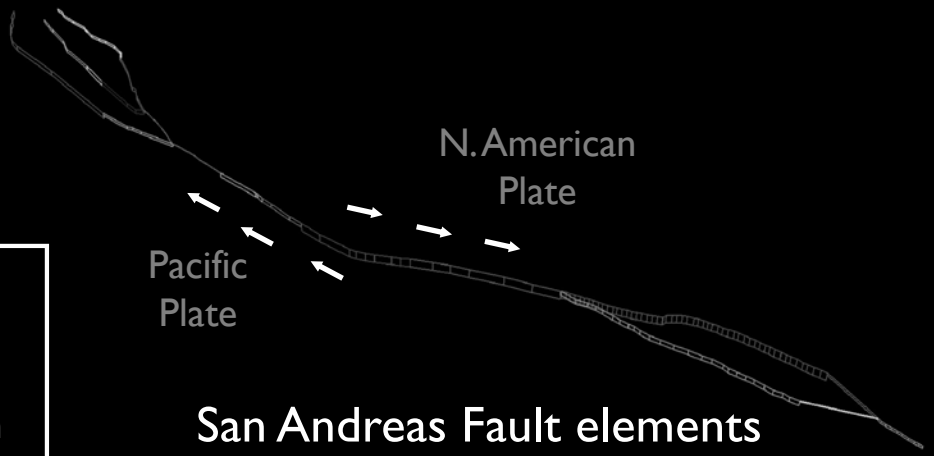

San Andreas Fault elements

Model efficiency

- 2048 x 2048 grid cells, 400 fault elements
- common locking depth, single event: ~ 1s of CPU time
- 27 locking depths, 70 events over 1000 years: < 30 min

Building a 4-D Model of the Earthquake Cycle

1. Physical model: 4-D Maxwell viscoelastic
2. Initial slip rate estimates (geology)
3. Crustal velocities (GPS/InSAR)
4. Historical earthquakes (earthquake record)
5. Pre-historical earthquakes and recurrence intervals (paleoseismology)

elastic

viscoelastic

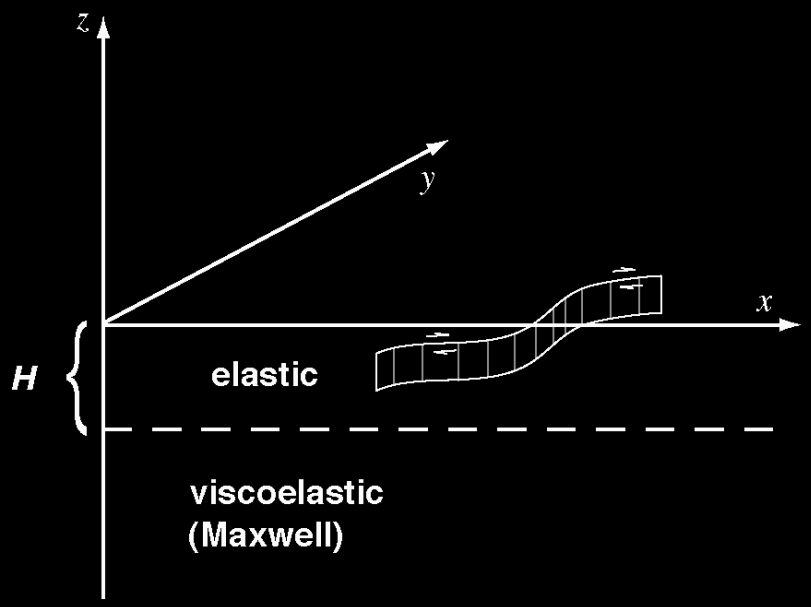

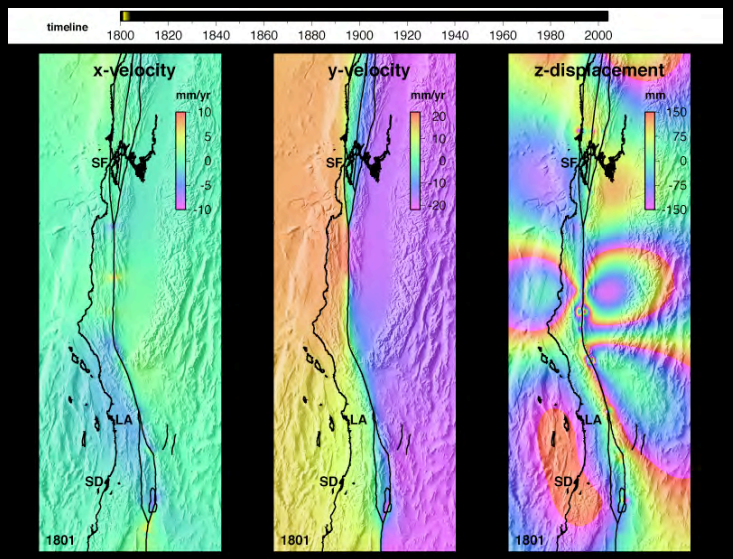

Geological Slip Rates

- Provides block motion
- Far-field velocity must match North America-Pacific plate motion (45 mm/yr)

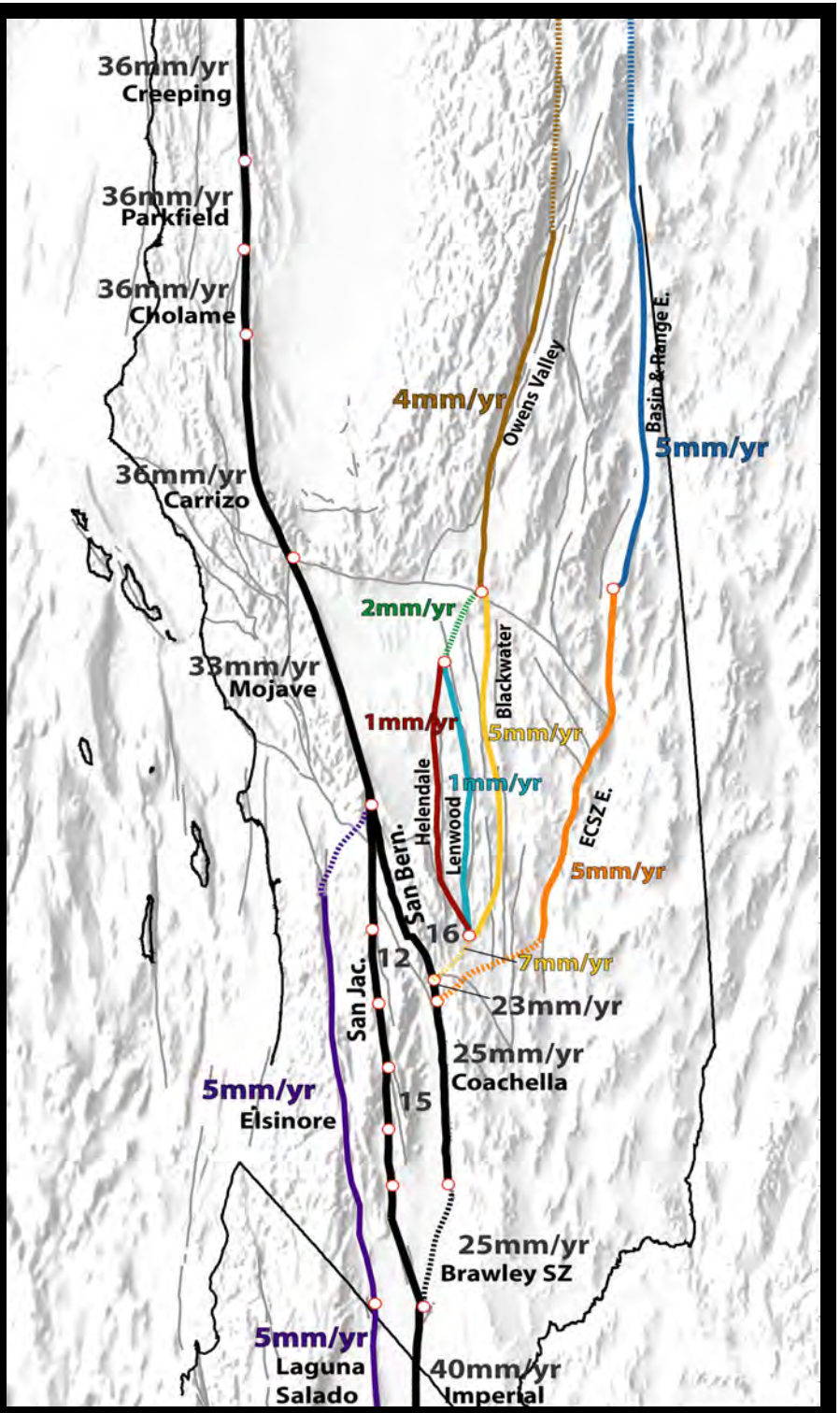

GPS data

[*Tong et al., JGR* 2013]

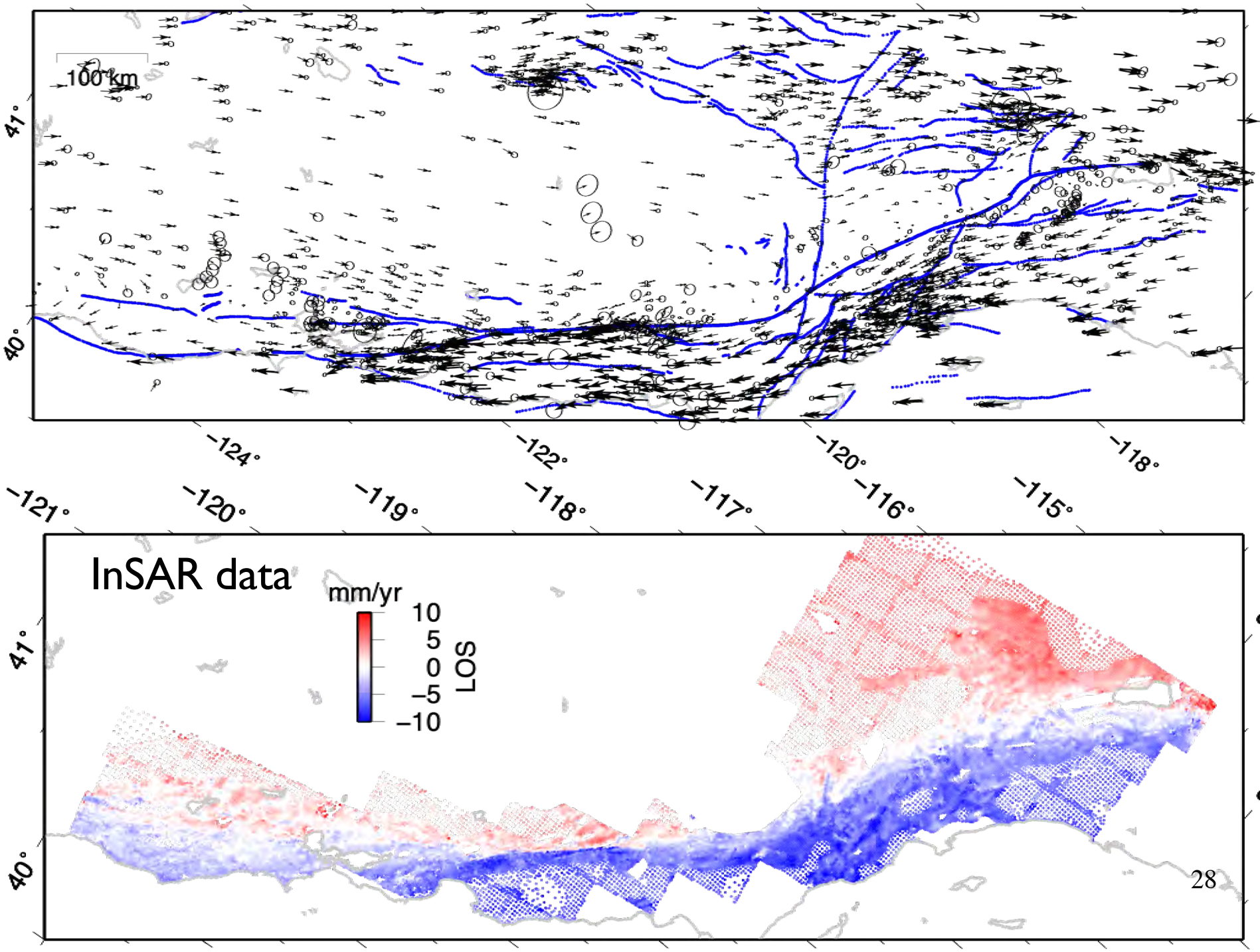

Historical Earthquakes

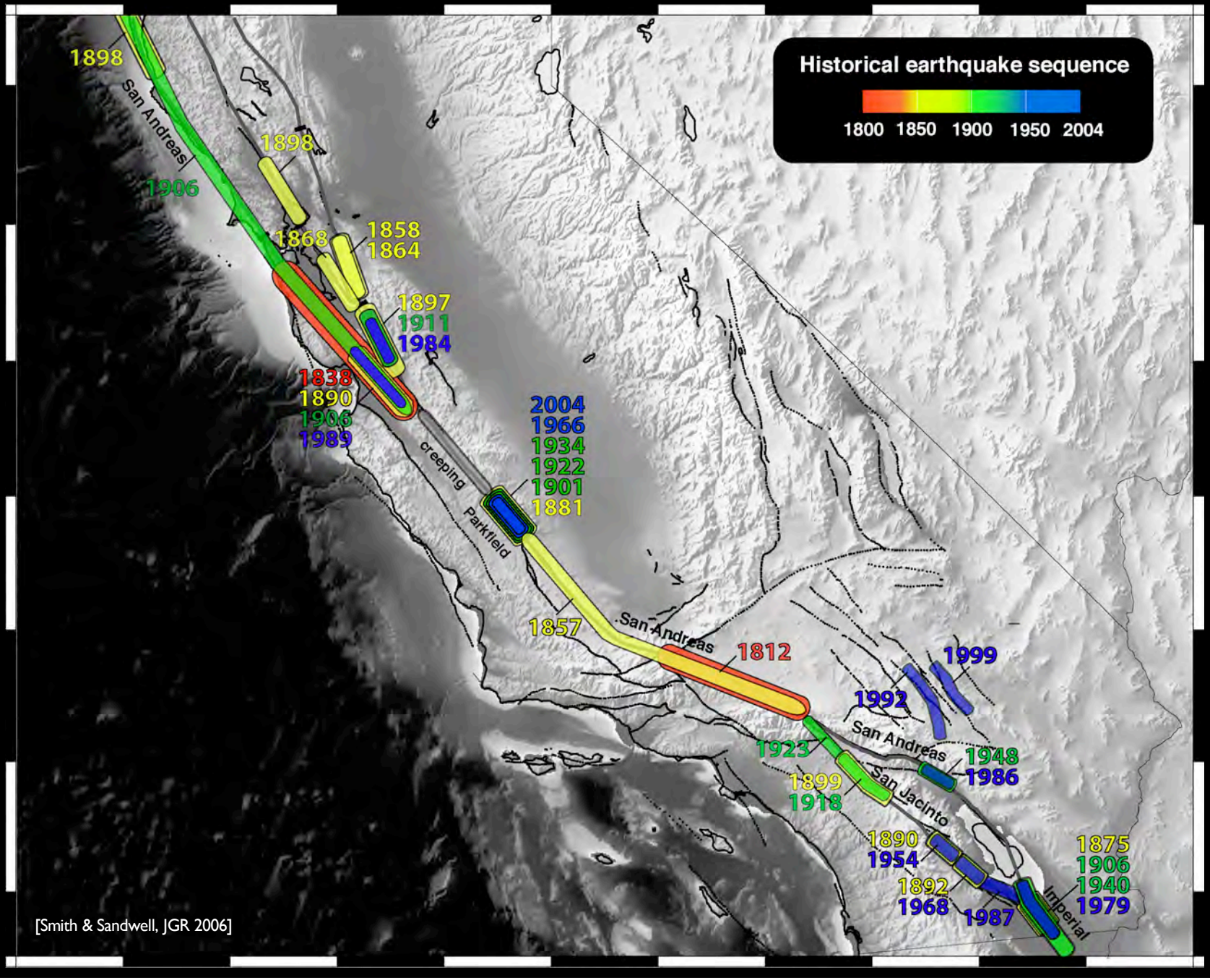

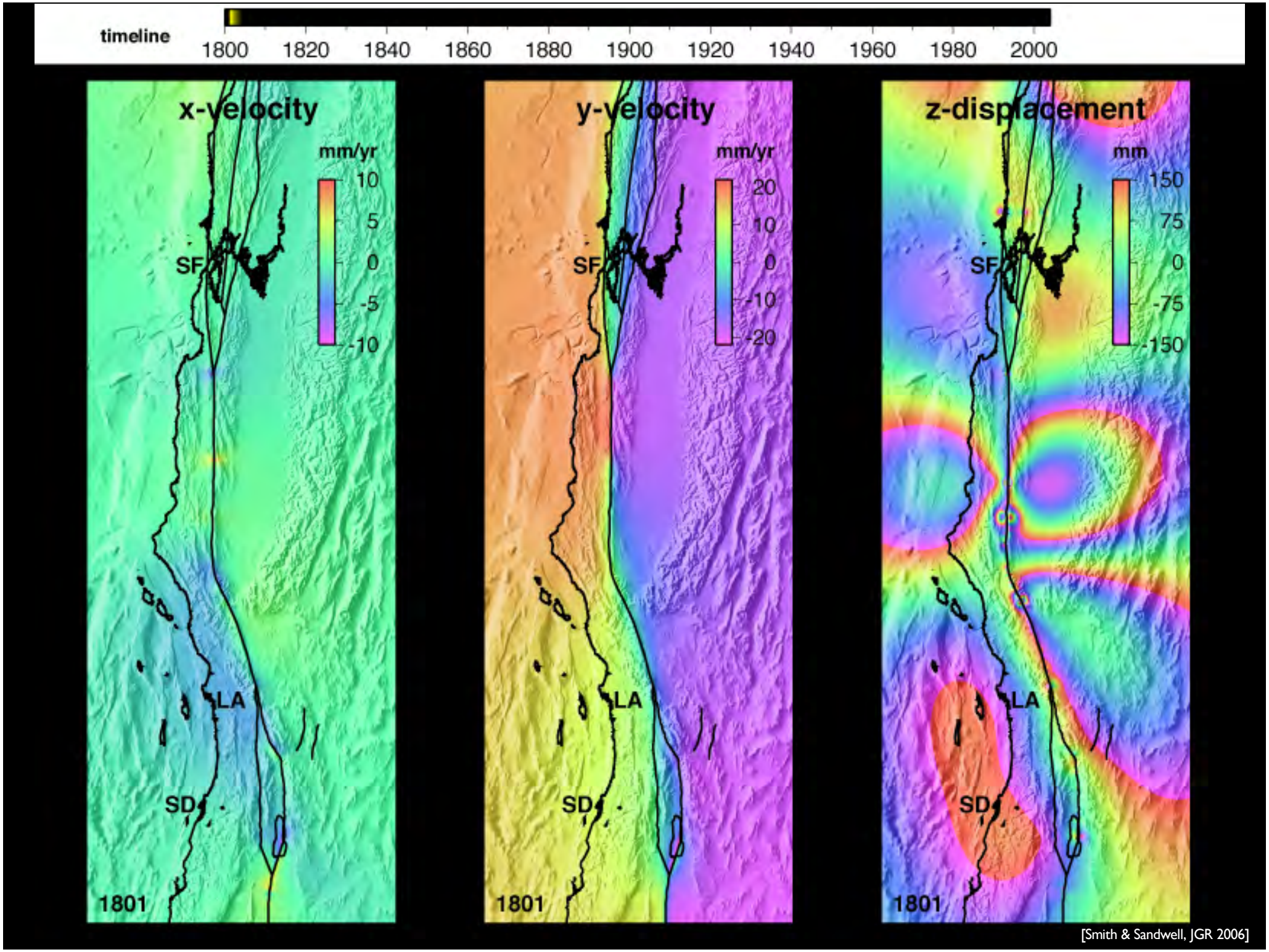

[Smith & Sandwell, JGR 2006]

3 candidate models

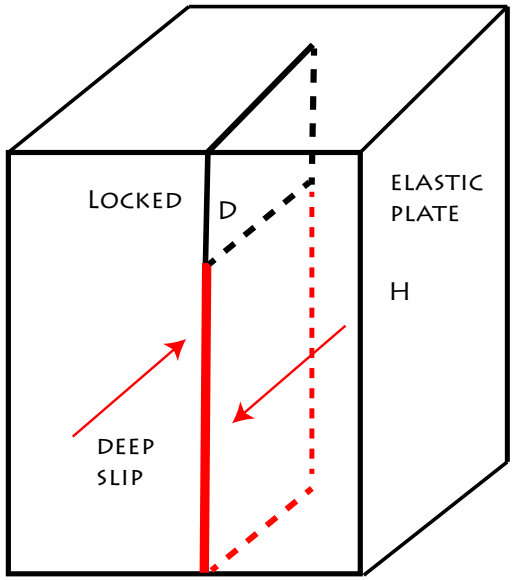

Half-space model
H=9999 km

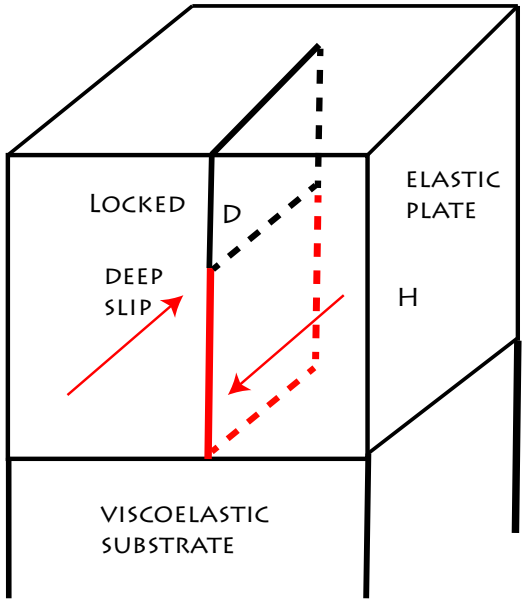

Thick plate model
H=60 km

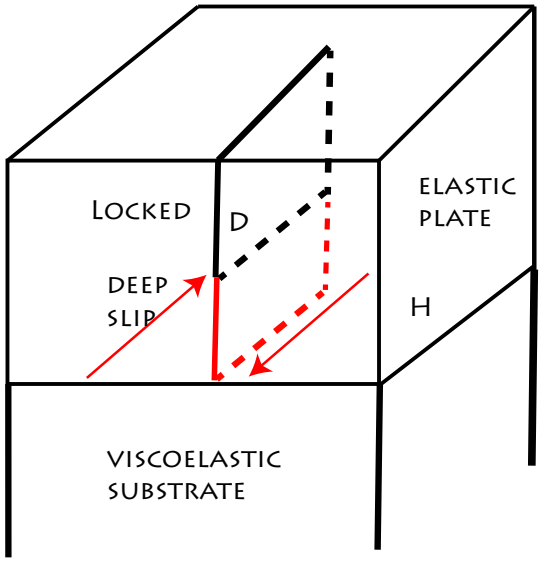

Thin plate model
H=30 km

None — Weak — Strong

Earthquake cycle effects

Inverse problem

- Green function
  - Deep slip in the **earthquake cycle model** $\overline{\overline{G_g}}$ $\overline{\overline{G_i}}$
  - Fault creep from layered elastic model $\overline{\overline{E_g}}$ $\overline{\overline{E_i}}$
- Geological constraint $\overline{\overline{C}}$
- Smoothing factor $\overline{\overline{S}}$
- Invert for:
  - deep slip rate $\bar{s}$
  - fault creep rate $\bar{p}$
- Data:
  - GPS $\overline{v_g}$
  - InSAR $\bar{l}$
  - Geological slip rate $\overline{s_c}$

$$\begin{bmatrix} \overline{\overline{G_g}} & \overline{\overline{E_g}} \\ \overline{\overline{G_i}} & \overline{\overline{E_i}} \\ \overline{\overline{C}} & 0 \\ 0 & \overline{\overline{S}} \end{bmatrix} \begin{bmatrix} \bar{s} \\ \bar{p} \end{bmatrix} = \begin{bmatrix} \overline{v_g} \\ \bar{l} \\ \overline{s_c} \\ 0 \end{bmatrix}$$

[*Tong et al.*, 2014]

GPS velocity for the thick plate

Observed calculated residual

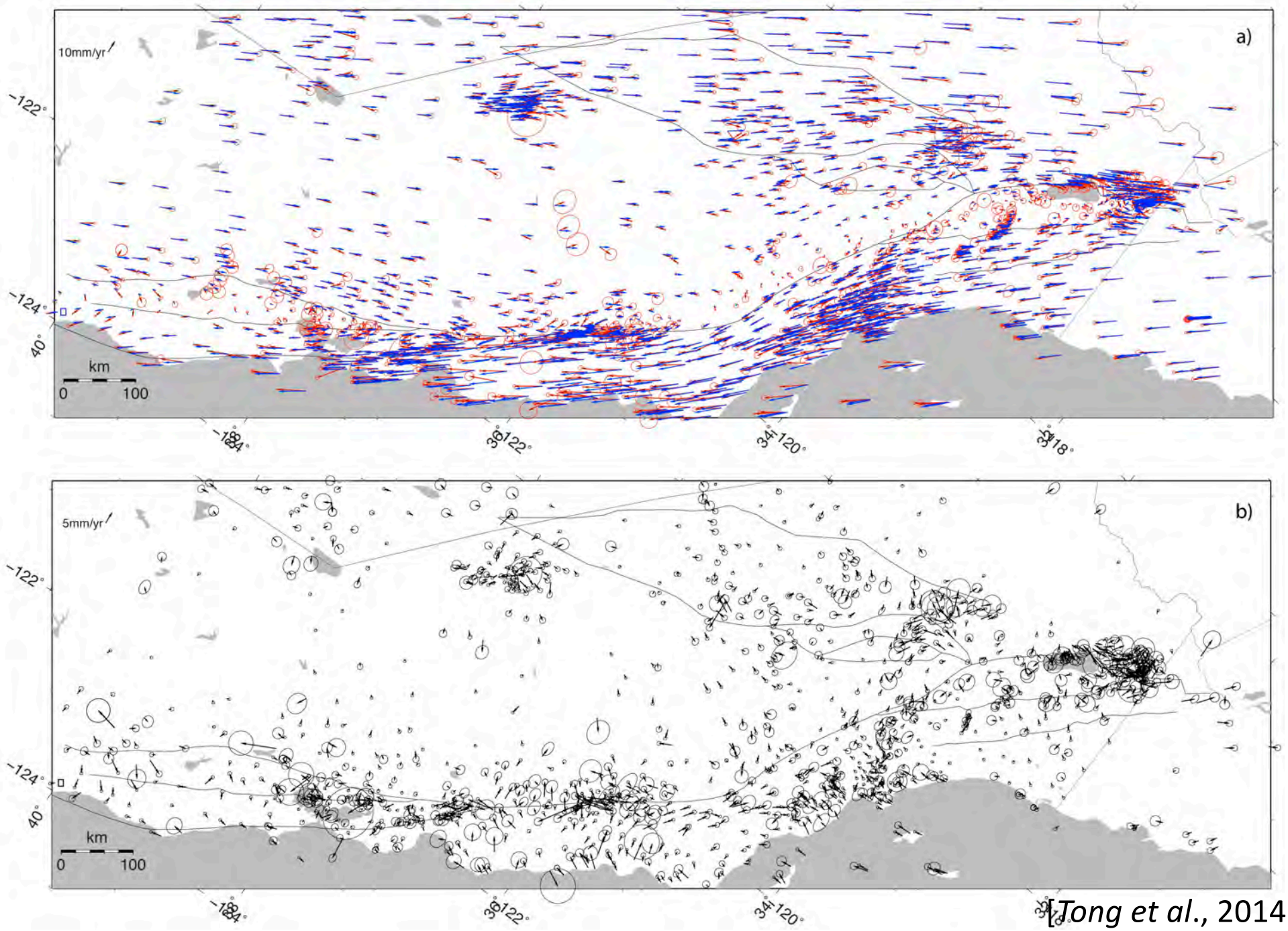

[*Tong et al.*, 2014]

InSAR velocity for the thick plate

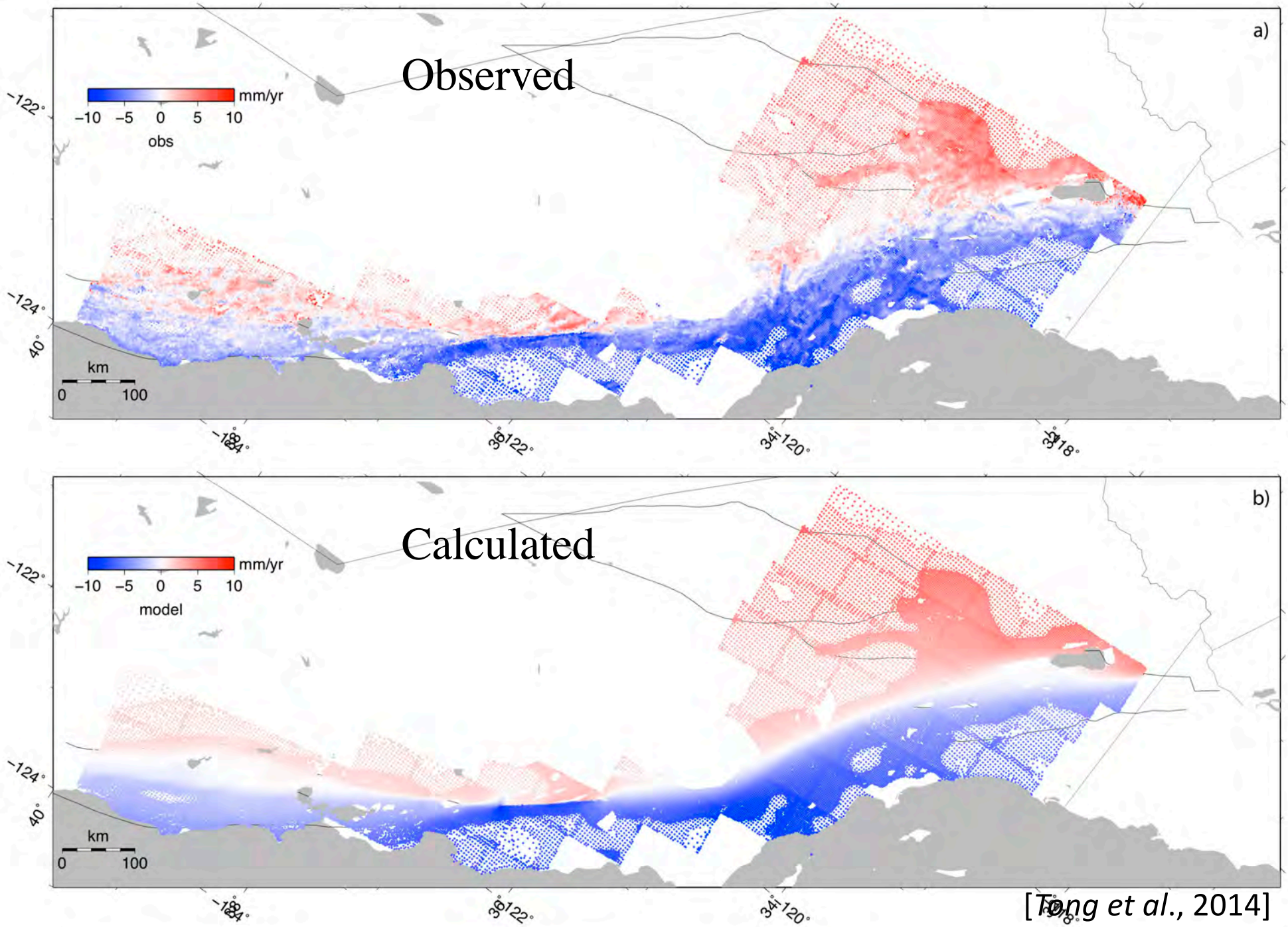

[*Tong et al.*, 2014]

present-day velocities and fit to GPS

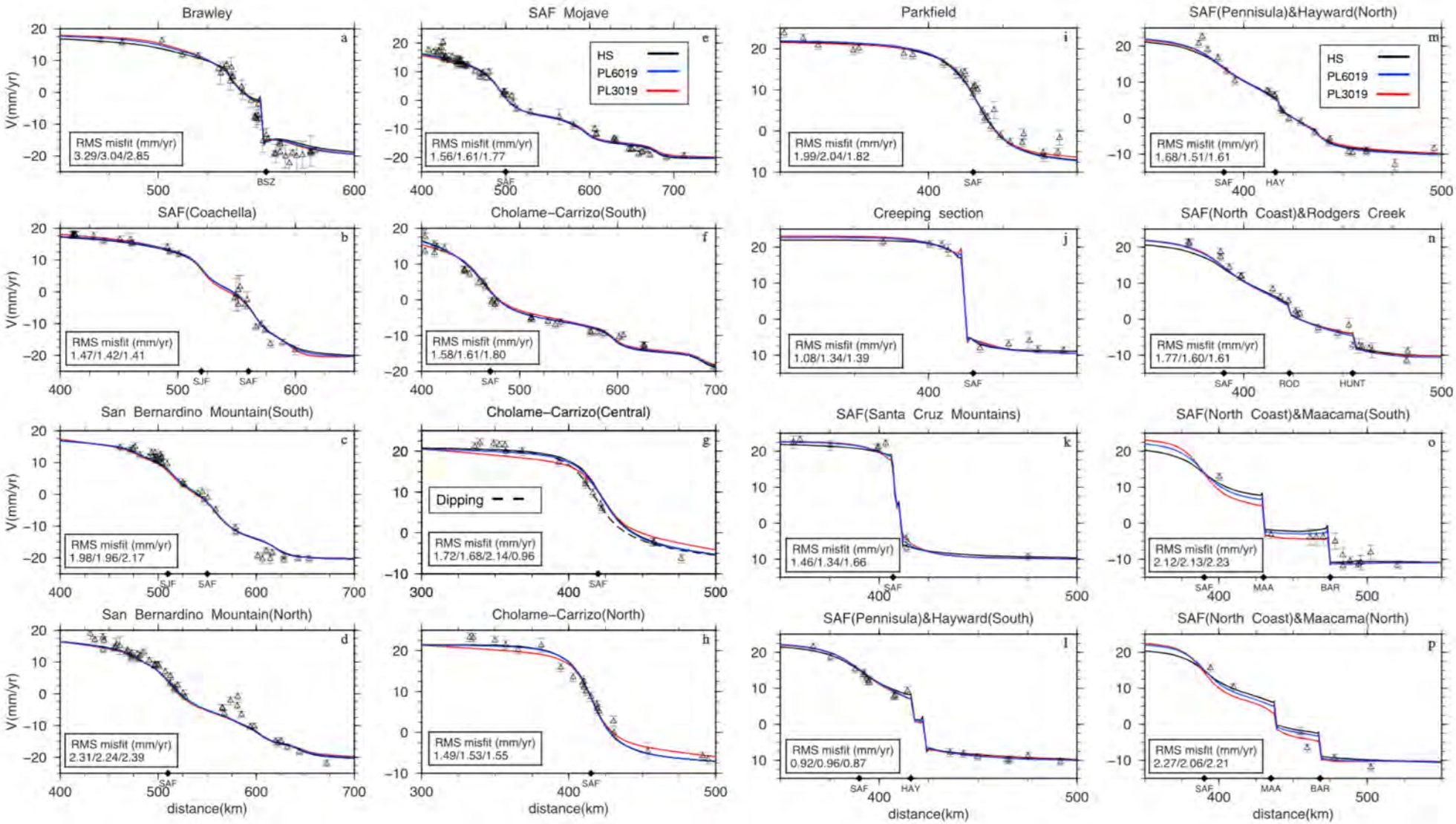

[*Tong et al.*, 2014]

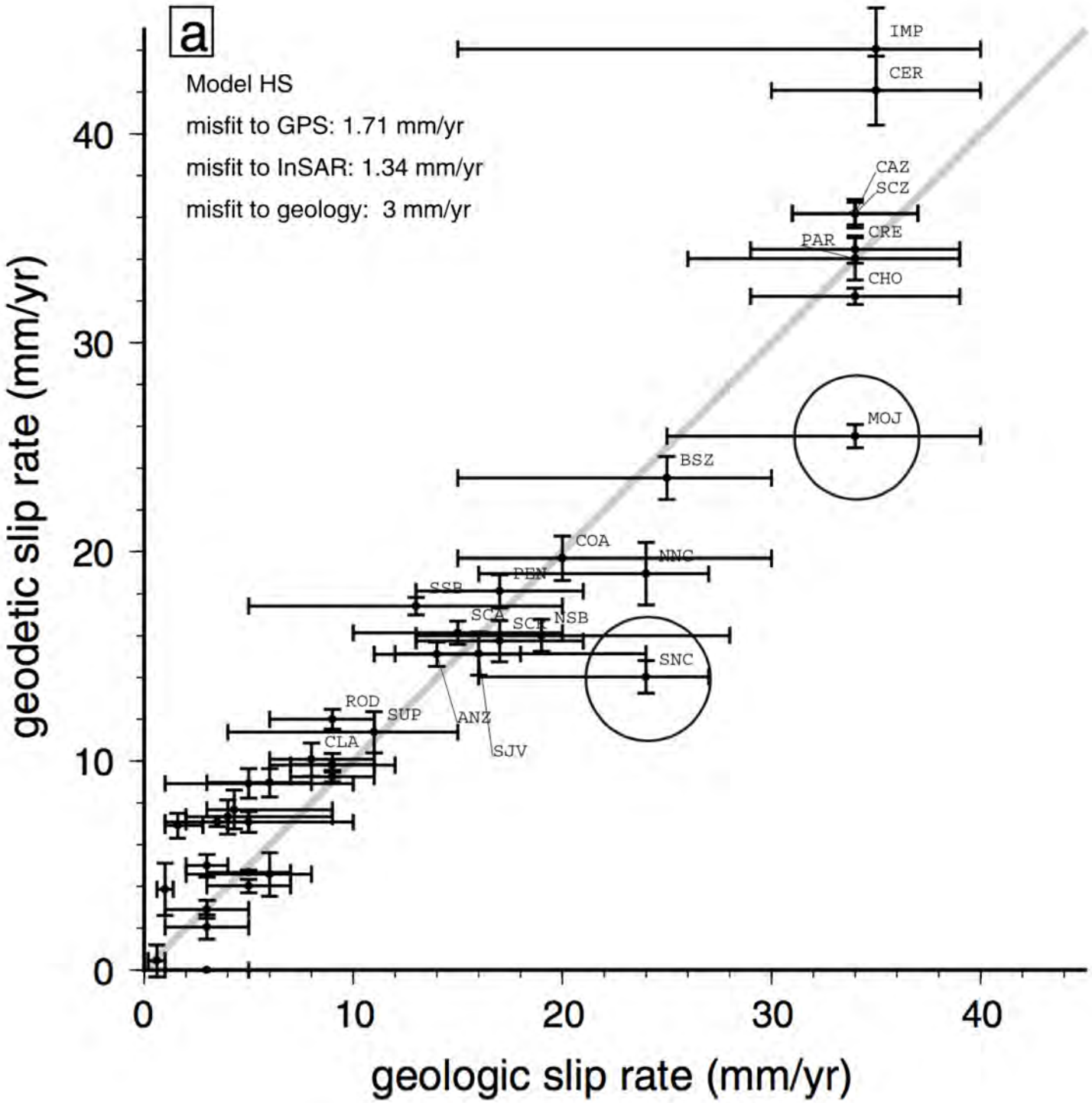

half space model

[*Tong et al.*, 2014]

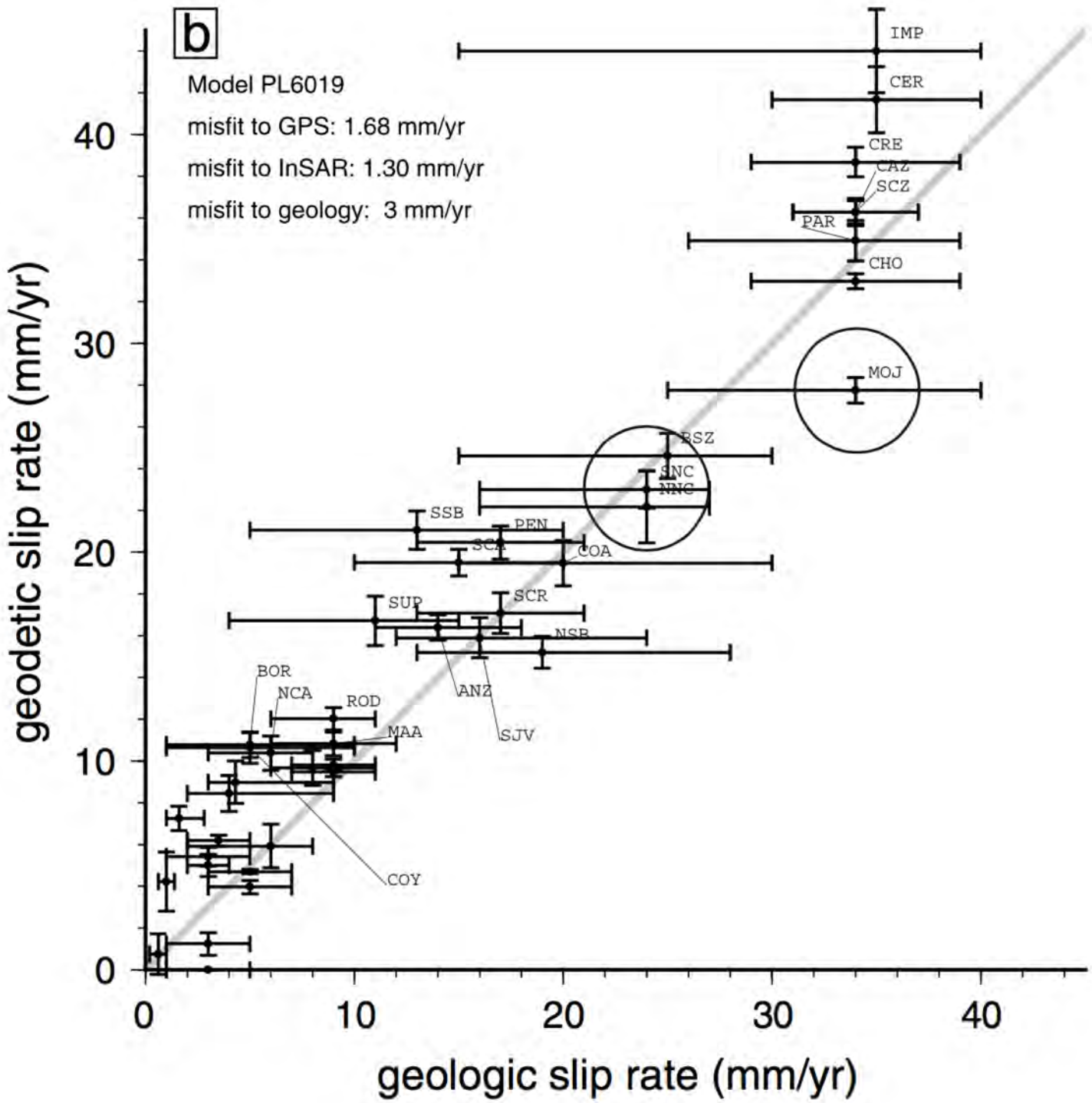

plate model

[*Tong et al.*, 2014]

Geodetic rate is within the error bounds of the geologic rate when a viscoelastic model is used. Agreement at Mojave segment was shown previously by *Chuang and Johnson*, [2011] and *Hearn et al.*, [2013].

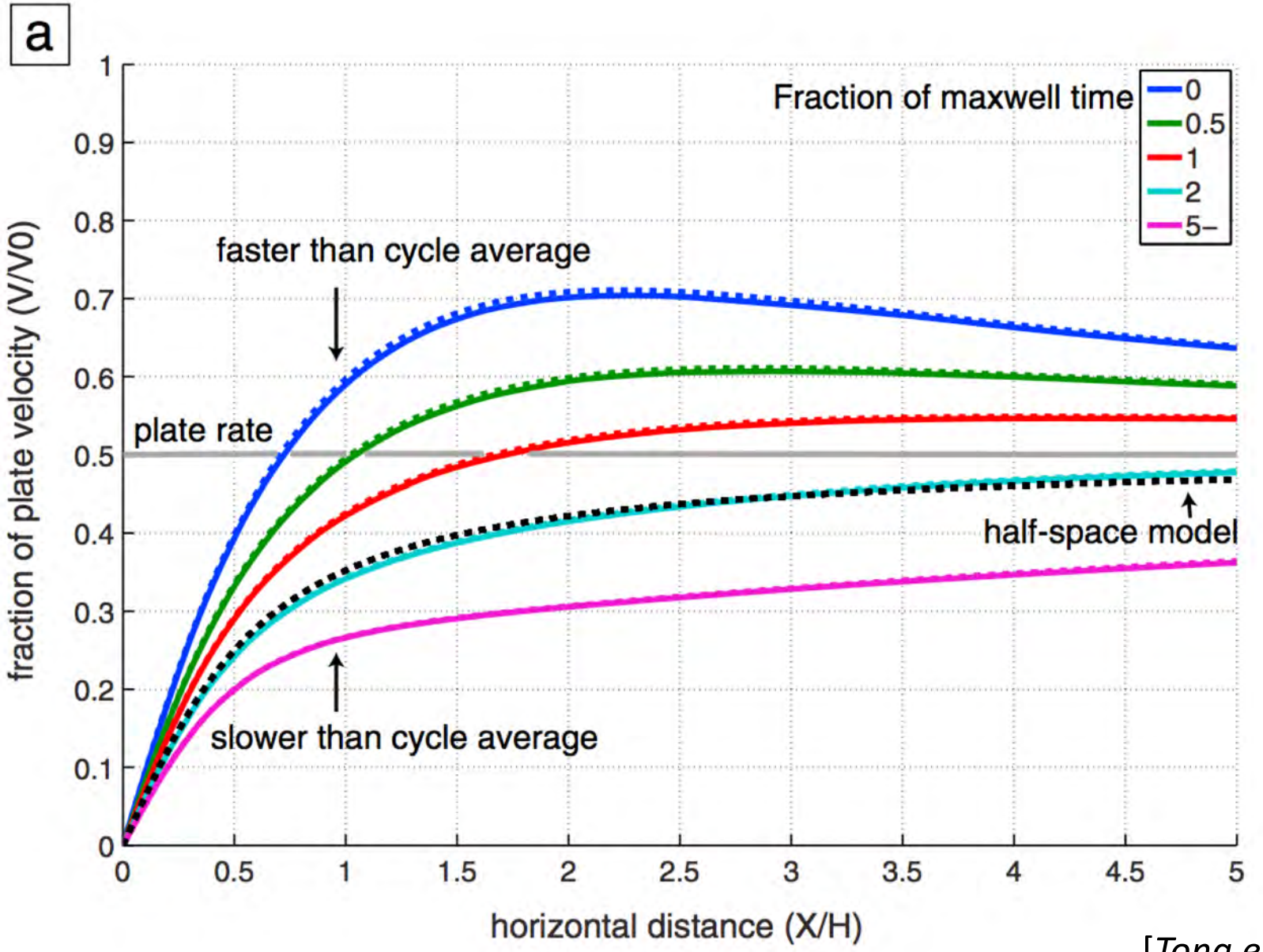

[*Tong et al.*, 2014]

4-D stress

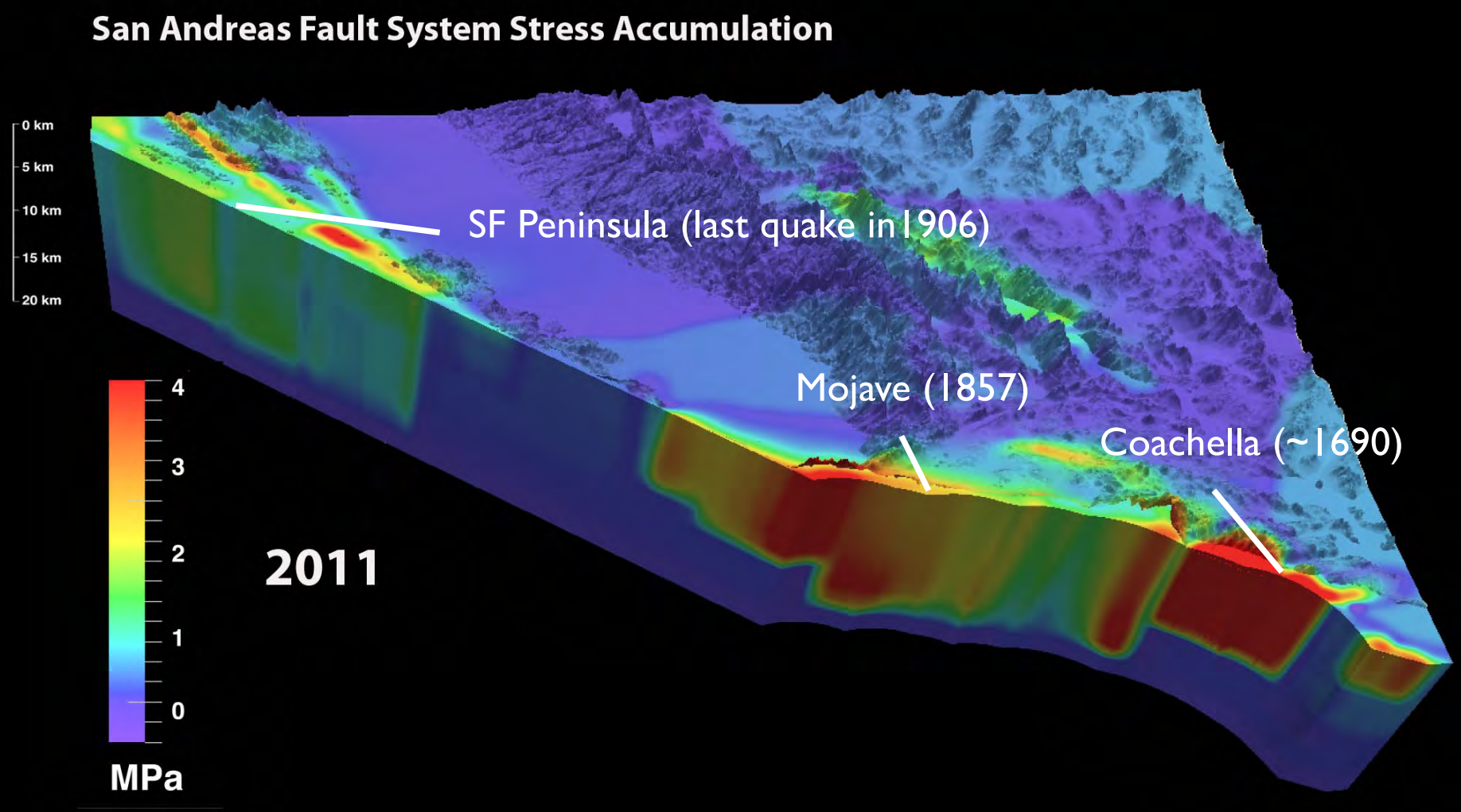

[Smith-Konter, AGU 2011]

Model of 4-D Stress

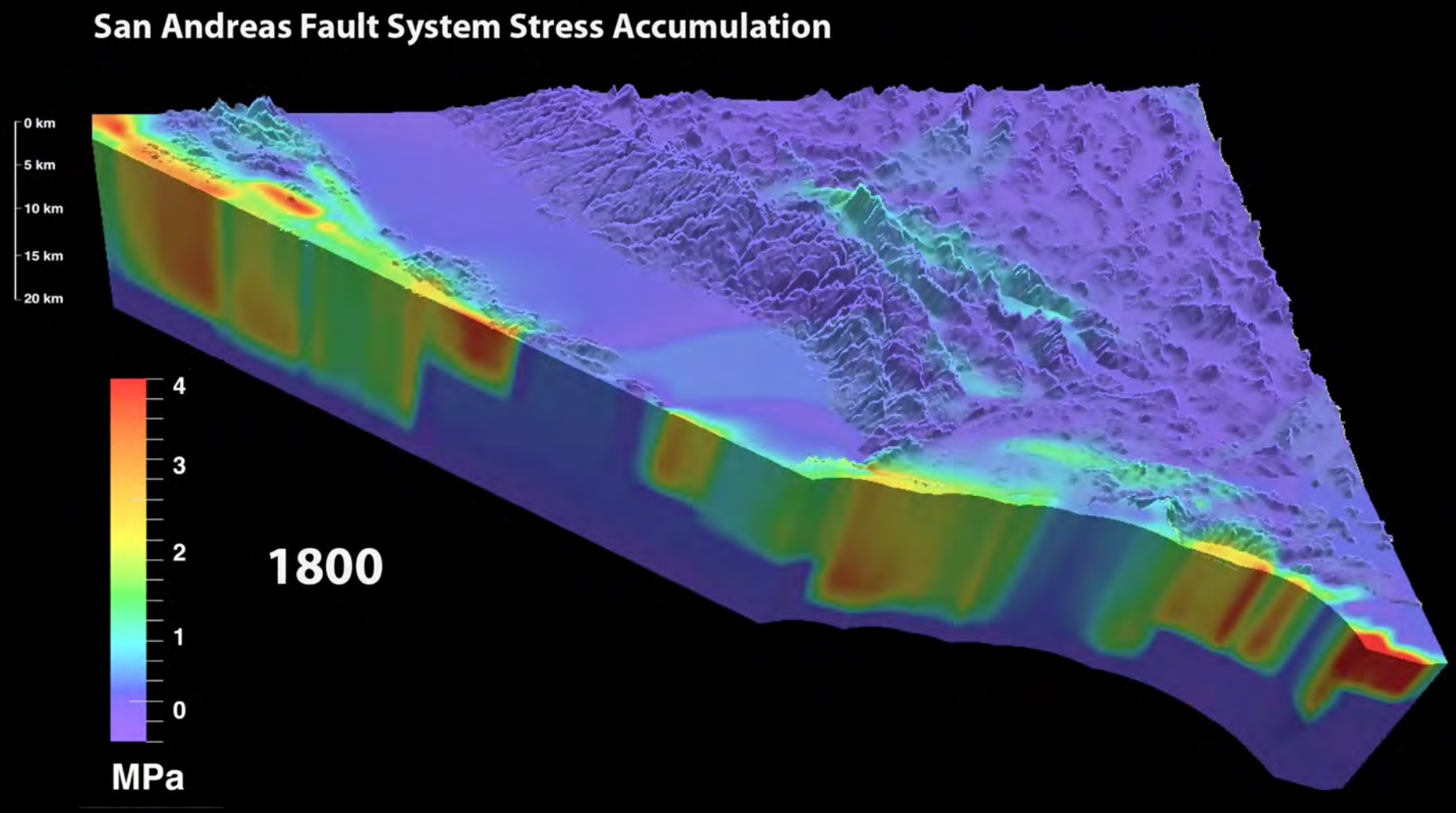

[Smith-Konter, AGU 2011]

Hindcast Stress Estimates: 1690, 1857, 1906

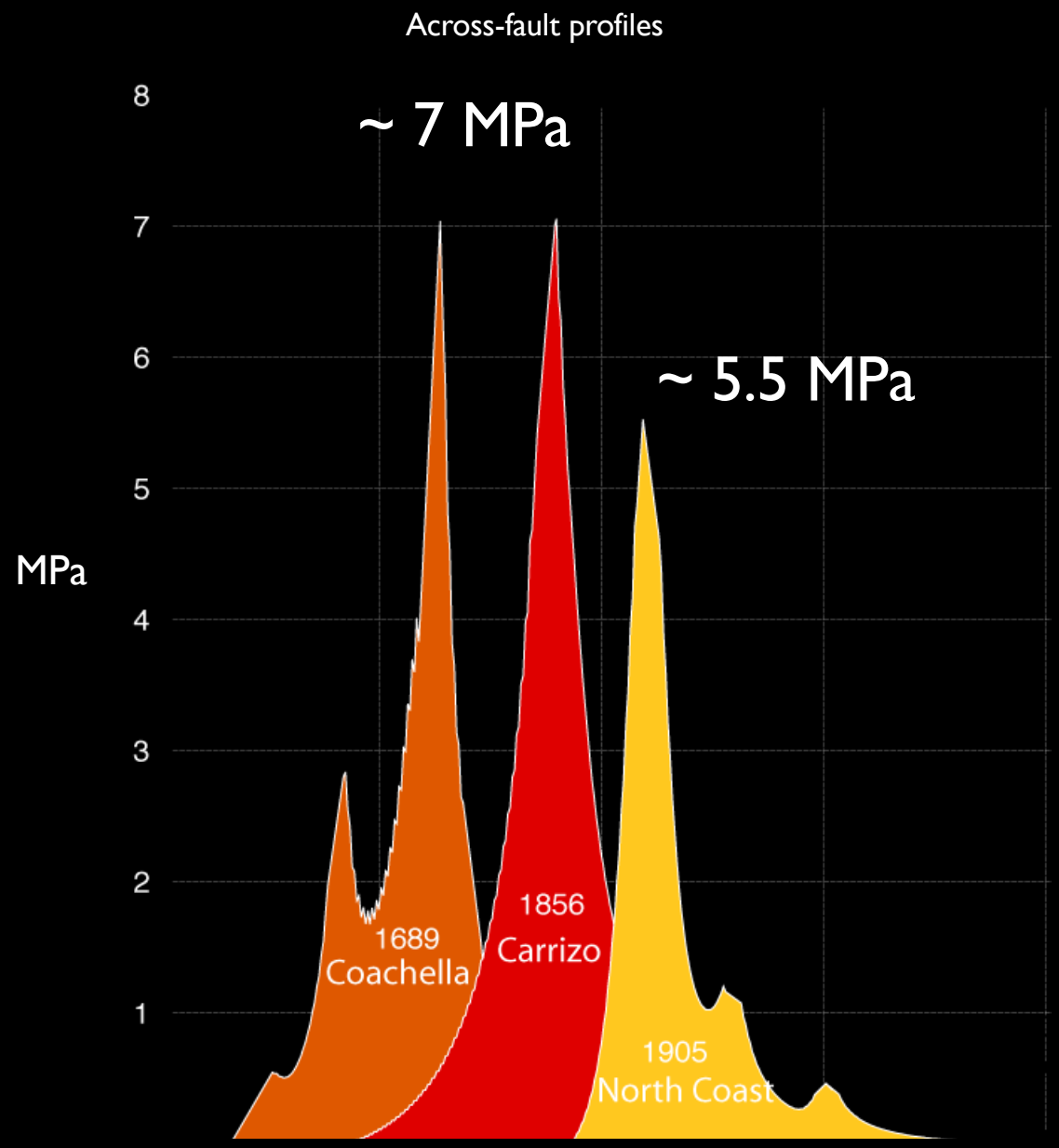

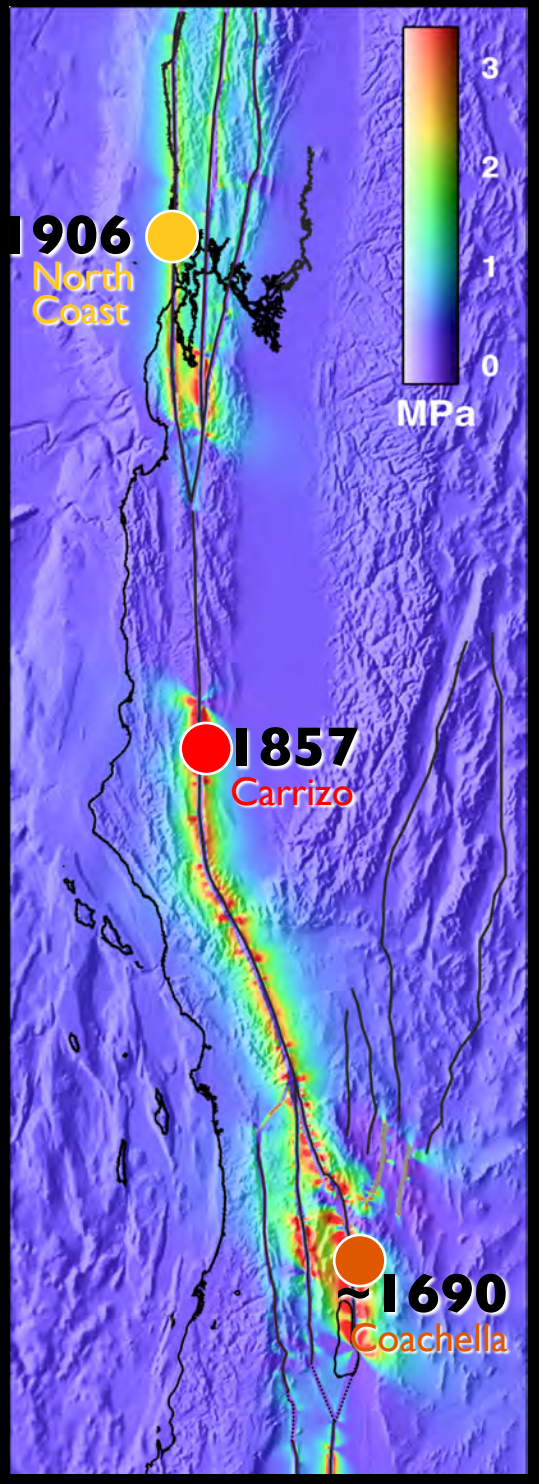

Hindcast Stress Estimates: North Coast Segment

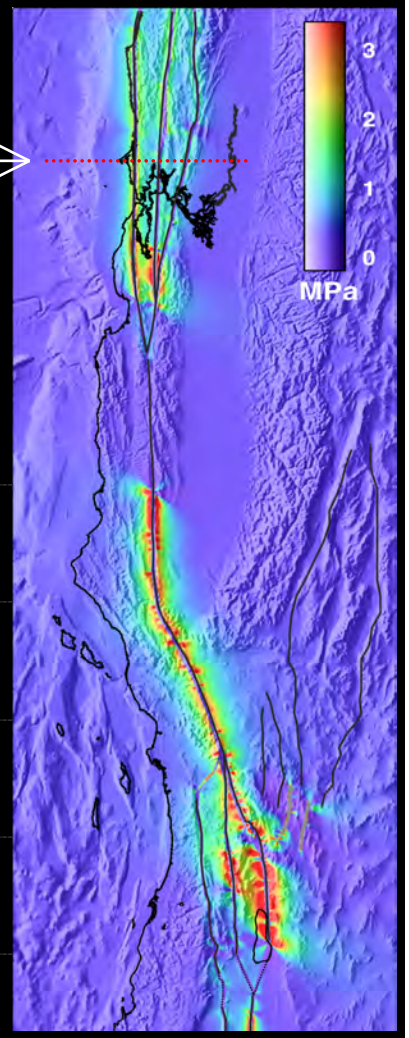

Across-fault profiles

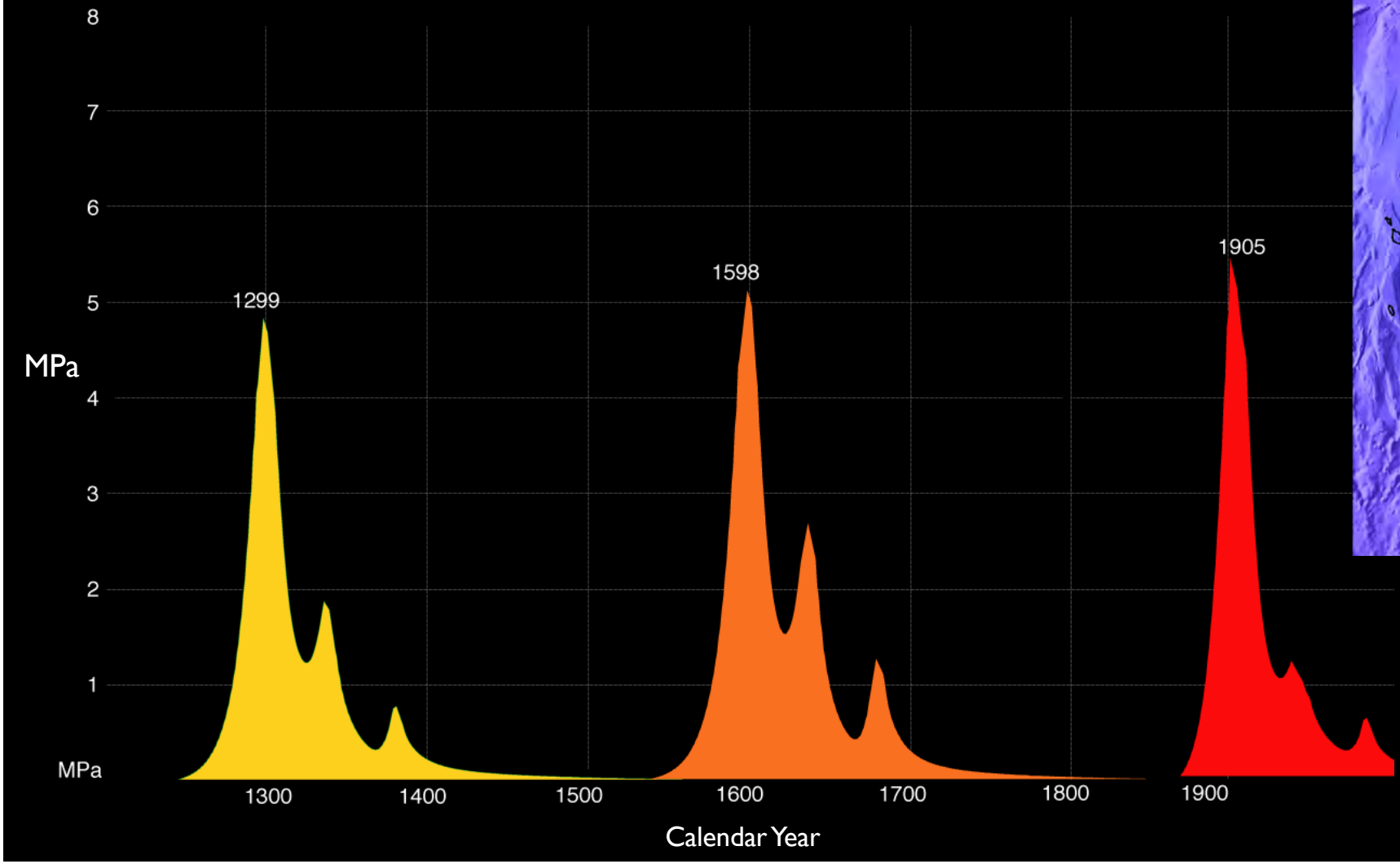

Hindcast Stress Estimates: Carrizo Segment

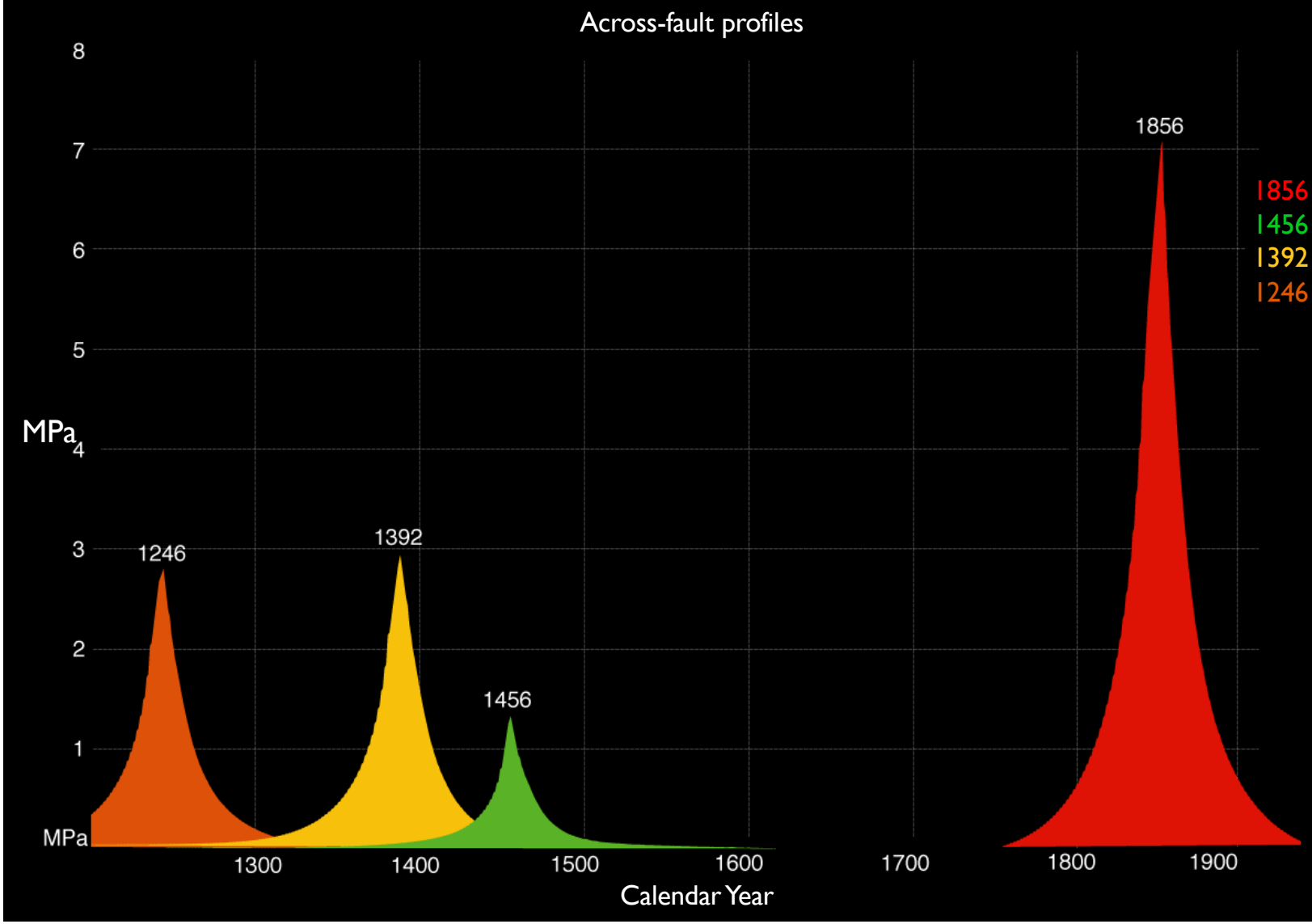

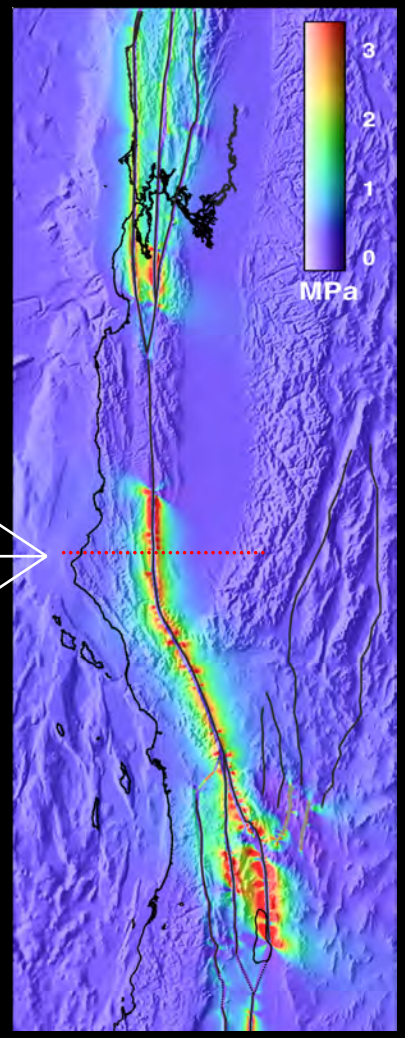

Stress Accumulation Time Series: Coachella Segment

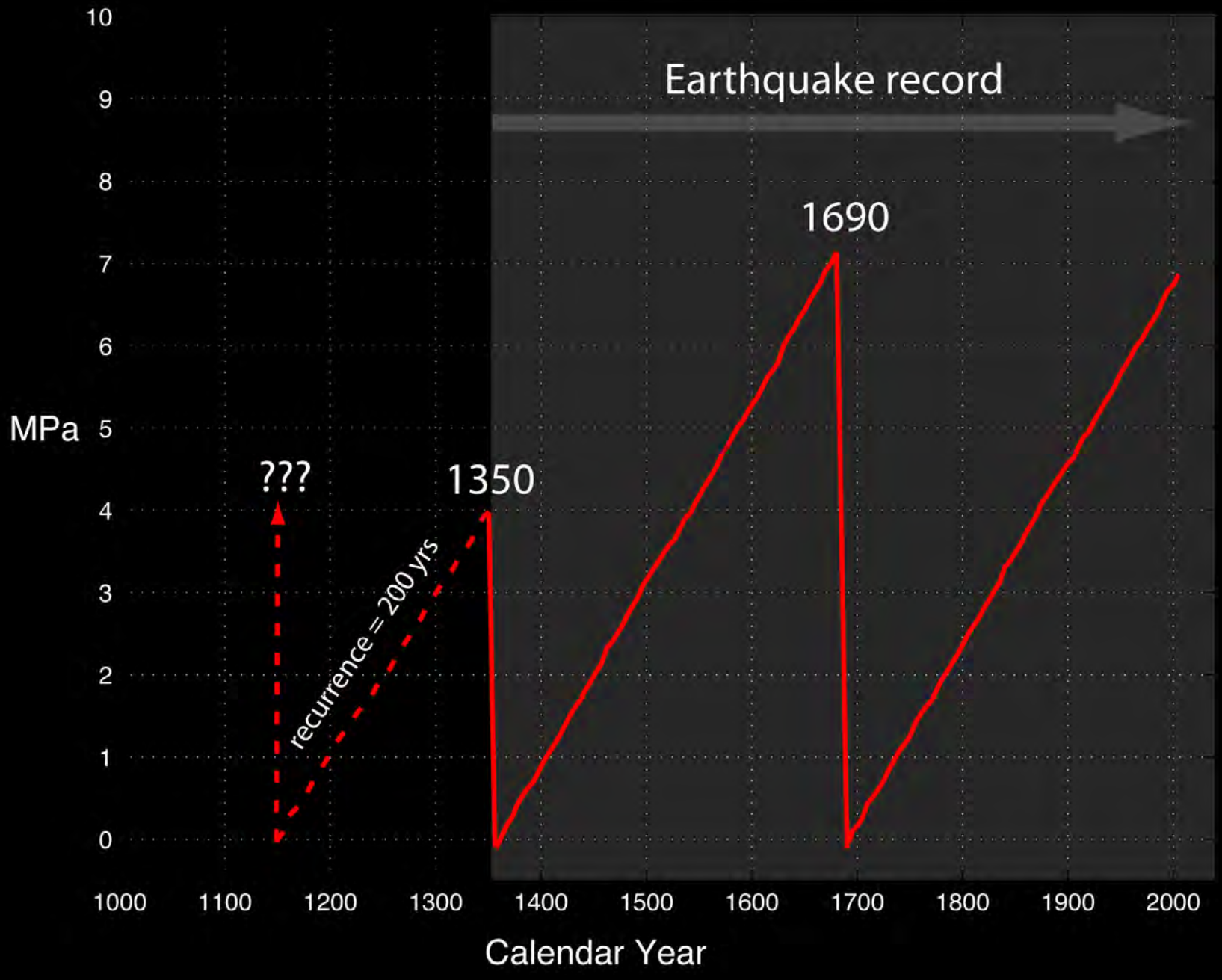

Hindcast Stress Estimates: Coachella Segment

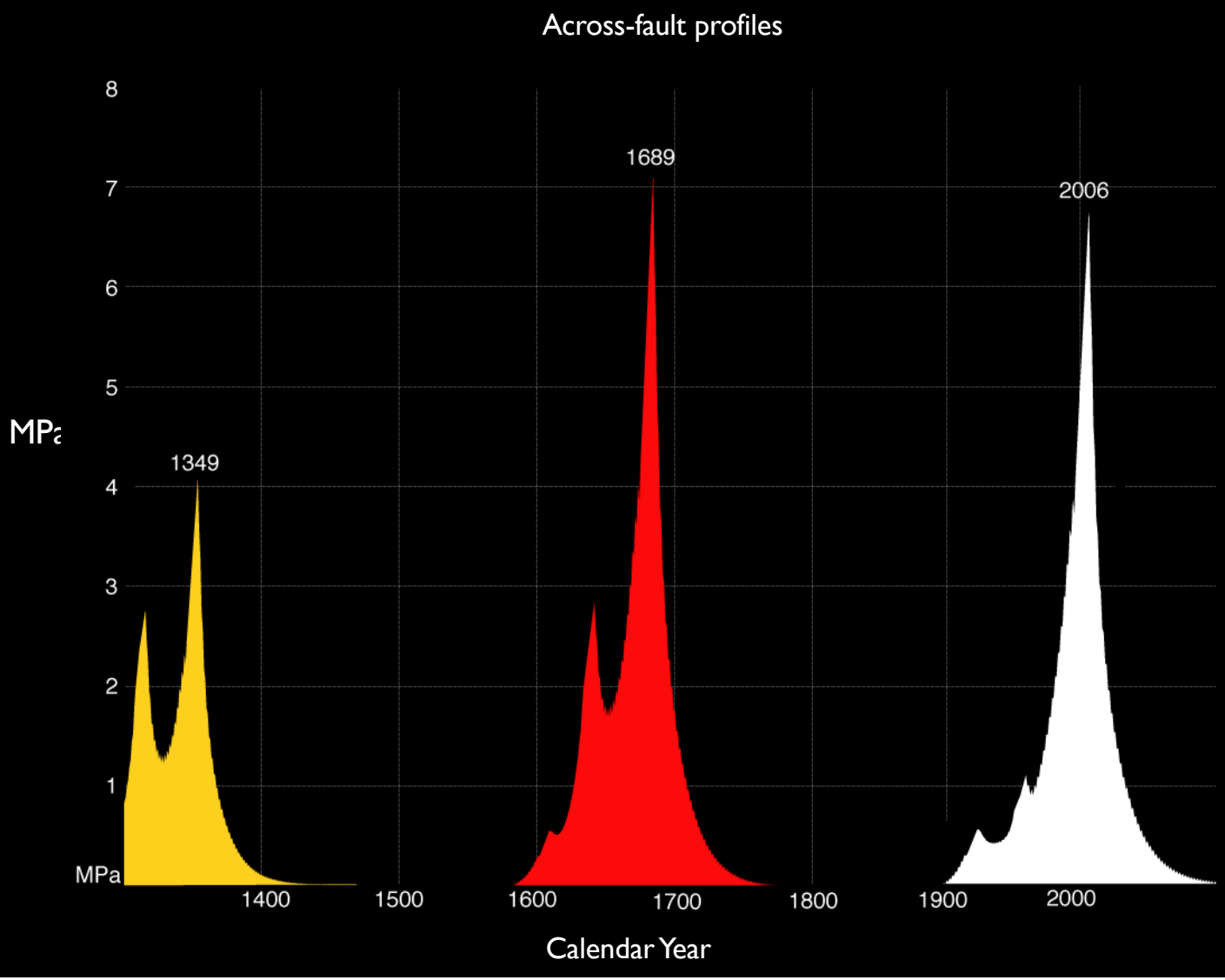

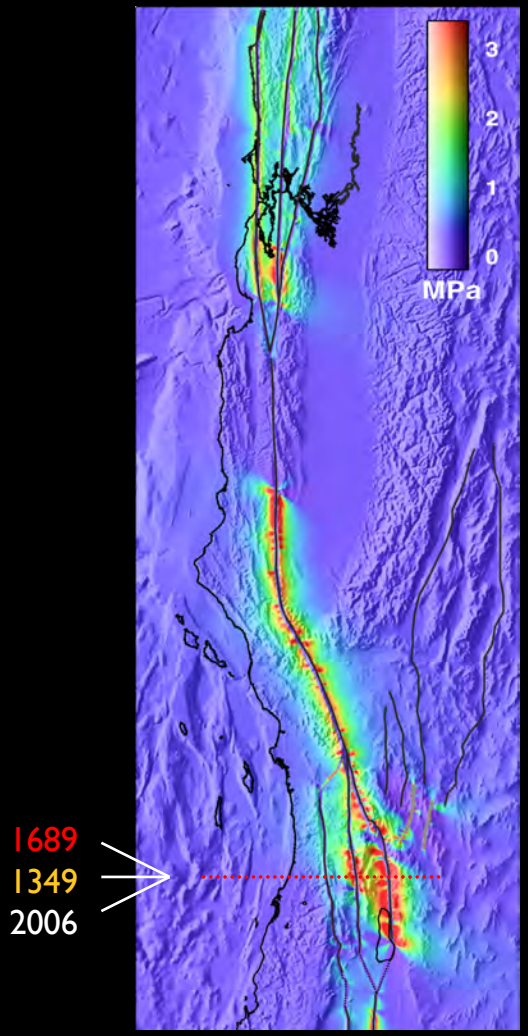

Past & Present Stress Estimates

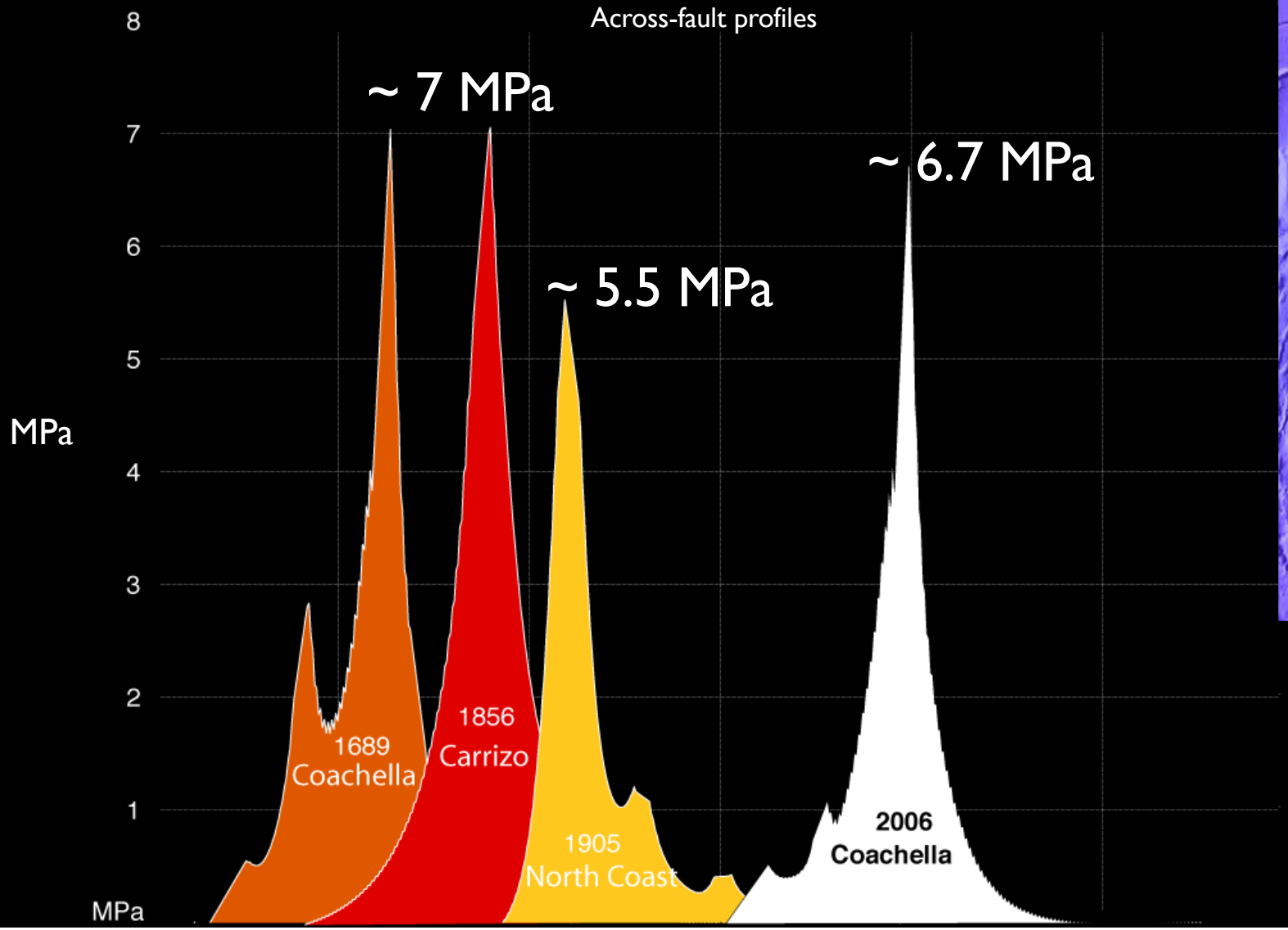

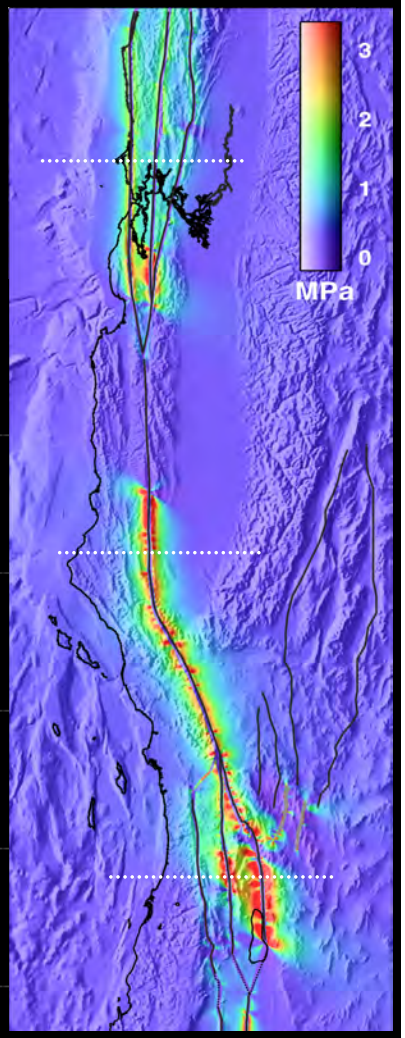

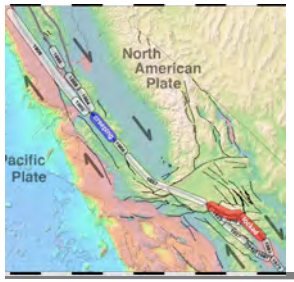

Conclusions

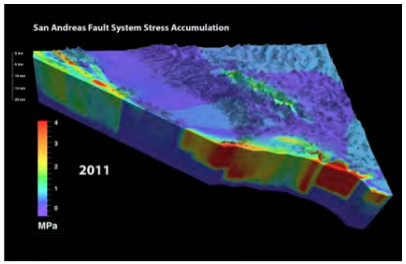

- Combined GPS (far-field) and InSAR (near field) provide a direct measure of moment accumulation rate.
- Block models do not include earthquake cycle effects and provide incorrect vertical motions.
- We have developed a semi-analytic 4-D earthquake cycle model that is fast enough for large-scale inversions with 2000 year simulations.
- Geodetic and geologic slip rates agree when earthquake cycle model is used.
- In the past earthquakes have occurred when the Coulomb stress reached ~7 MPa.
- ALOS-2 and Sentinel-1 will are providing a second InSAR look direction for tighter bounds on moment accumulation rate.
- code available at http://topex.ucsd.edu/body_force